data by non-linear regression using Prism (GraphPad Software, San Diego, CA, USA) to calculate E_{max} and EC_{50} values. EC_{50} values were used to compare the relaxant effects of the cGMP analogues. A *t*-test was used to assess the significance of differences between EC_{50} values. A *P*-value <0.05 was taken to indicate a statistically significant difference. Statistical analysis was performed using Prism software.

Materials

8-Nitro-cGMP and 8-bromo-cGMP were synthesized as described previously (Sawa *et al.*, 2007). Phenylephrine hydrochloride (Phe), ACh, a NOS inhibitor N^{ω}-nitro-L-arginine methyl ester (L-NAME), a superoxide scavenger SOD (from bovine erythrocytes), a SOD mimetic tiron (4,5-dihydroxy-1,3-benzene-disulphonic acid) (Mohazzab *et al.*, 1994), a cGMP-specific phosphodiesterase (PDE) inhibitor zaprinast and DHE were obtained from Wako Pure Chemical Industries (Osaka, Japan). Iberiotoxin was purchased from Peptide Institute Inc. (Osaka, Japan). Preparations of all stock solutions and their subsequent dilution were made using distilled water. Exceptions to this were zaprinast and DHE, which were dissolved in DMSO (0.1% final concentration). As a control, some aortas were treated with DMSO (0.1%) alone and no changes were observed.

Results

Effects of 8-nitro-cGMP on Phe-induced contraction in C57BL/6 mouse aorta

8-Nitro-cGMP by itself did not induce any significant change in basal tone of thoracic aortic rings from wild-type C57BL/6 mice (not shown). However, in the aortas contracted with the α-adrenoceptor agonist Phe (0.1 μM), 8-nitro-cGMP induced dose-dependent changes in isometric tension. As shown in Figure 1A, the cumulative addition of 0.001–100 μM 8-nitro-cGMP produced a biphasic effect: at concentrations up to 10 μM the increase in tension of the Phe-contracted aortas was statistically significant, and at higher than 10 μM the contracted rings were dose-dependently relaxed. A cell-permeable cGMP analogue, 8-bromo-cGMP induced only dose-dependent relaxation in the aortas contracted with Phe (not shown).

The relaxation induced by 8-nitro-cGMP at higher than 10 μM in the aortas from C57BL/6 mouse was decreased by 25% after pretreatment of the aortas with a BK-type Ca^{2+}-activated K^+ channel blocker, iberiotoxin (100 nM) (results not illustrated).

Inhibitory effects of L-NAME and superoxide scavenger on 8-nitro-cGMP-induced enhancement of contraction to Phe in C57BL/6 mouse aorta

We have previously reported that mechanical removal of the endothelium in SD rat carotid artery significantly attenuates the 8-nitro-cGMP-enhanced contraction to Phe (Sawa *et al.*, 2007). To determine the involvement of eNOS in 8-nitro-cGMP-induced enhancement of contraction to Phe in mouse aortas, we examined the effects of L-NAME, an inhibitor of NOS, on the 8-nitro-cGMP-induced enhancement. As shown in Figure 1A, pretreatment of aortas with 100 μM L-NAME abolished 8-nitro-cGMP-induced enhancement of the contraction to Phe.

Our previous studies had demonstrated superoxide formation in response to 8-nitro-cGMP by use of electron spin resonance spectroscopy (Sawa *et al.*, 2007). To further investigate the involvement of superoxide in the 8-nitro-cGMP-enhanced contractile responses, we examined the effects of the ROS scavenger, SOD and a SOD mimetic, tiron, on this response to 8-nitro-cGMP. In our preliminary experiments with aortas from C57BL/6 mice, Phe-induced contraction was attenuated by SOD (100 $U \cdot mL^{-1}$) or tiron (1 mM) (to 18% of contraction to Phe). As shown in Figure 1B, pretreatment of aortas from C57BL/6 mice with 100 $U \cdot mL^{-1}$ SOD abolished 8-nitro-cGMP-induced enhancement of the contraction to Phe. The potency of 1 mM tiron in the aortas was similar to that of SOD.

Involvement of eNOS uncoupling in 8-nitro-cGMP-enhanced contraction

To assess the possibility that 8-nitro-cGMP disrupts the eNOS dimer in aortas from C57BL/6 mice, we used low-temperature SDS-PAGE Western blots to characterize the dimer and monomer of eNOS in the aortic segments incubated with buffer alone, 8-nitro-cGMP or 8-bromo-cGMP at 10 μM for 30 min respectively. As shown in Figure 2A, the 8-nitro-cGMP-treated aortas were found to have a significant decrease in eNOS dimer/monomer ratio as assessed by the relative band density of the expected 280 KDa (dimer) and 140 KDa (monomer) immunoreactive bands. SDS-PAGE revealed that there was no difference in total eNOS expression in each aorta.

To visualize vascular superoxide production in response to 8-nitro-cGMP, we performed DHE fluorescence staining of frozen section aortas. As shown in Figure 2B, incubation of the aortas with 8-nitro-cGMP at 10 μM for 30 min significantly increased superoxide production, compared with 8-bromo-cGMP.

Vascular reactivity in diabetic mouse aorta

An important role of ROS contributing to the impaired regulation of arteriolar tone has recently received considerable attention in type 2 diabetes. Thus, we investigated the effects of 8-nitro-cGMP on isometric tension of aortas from type 2 diabetic db/db mice. The db/db mice at 13–14 weeks of age weighed more than their age-matched db/+ mice (db/db group: 48.85 ± 1.14 g; db/+ group: 29.5 ± 0.9 g; n = 10–12) with higher levels of blood glucose and plasma insulin (Dong *et al.*, 2010).

Contractility of thoracic aortas to high K^+ solution was not significantly different in db/db and db/+ mice (db/db group: 0.215 ± 0.007 g; db/+ group: 0.235 ± 0.009 g; n = 10–12). By contrast, the force generated in response to Phe (0.1 μM) was markedly greater in db/db aortas (Figure 3A). ACh-induced relaxations of db/db aortas contracted with Phe (0.1 μM) were significantly reduced compared with their respective controls (Figure 3B; db/db: E_{max} = 76.1 ± 4.6%, EC_{50} = 105.6 nM; db/+: E_{max} = 90.1 ± 1.8%, EC_{50} = 39.5 nM; n = 6). The endothelium-independent vasodilator

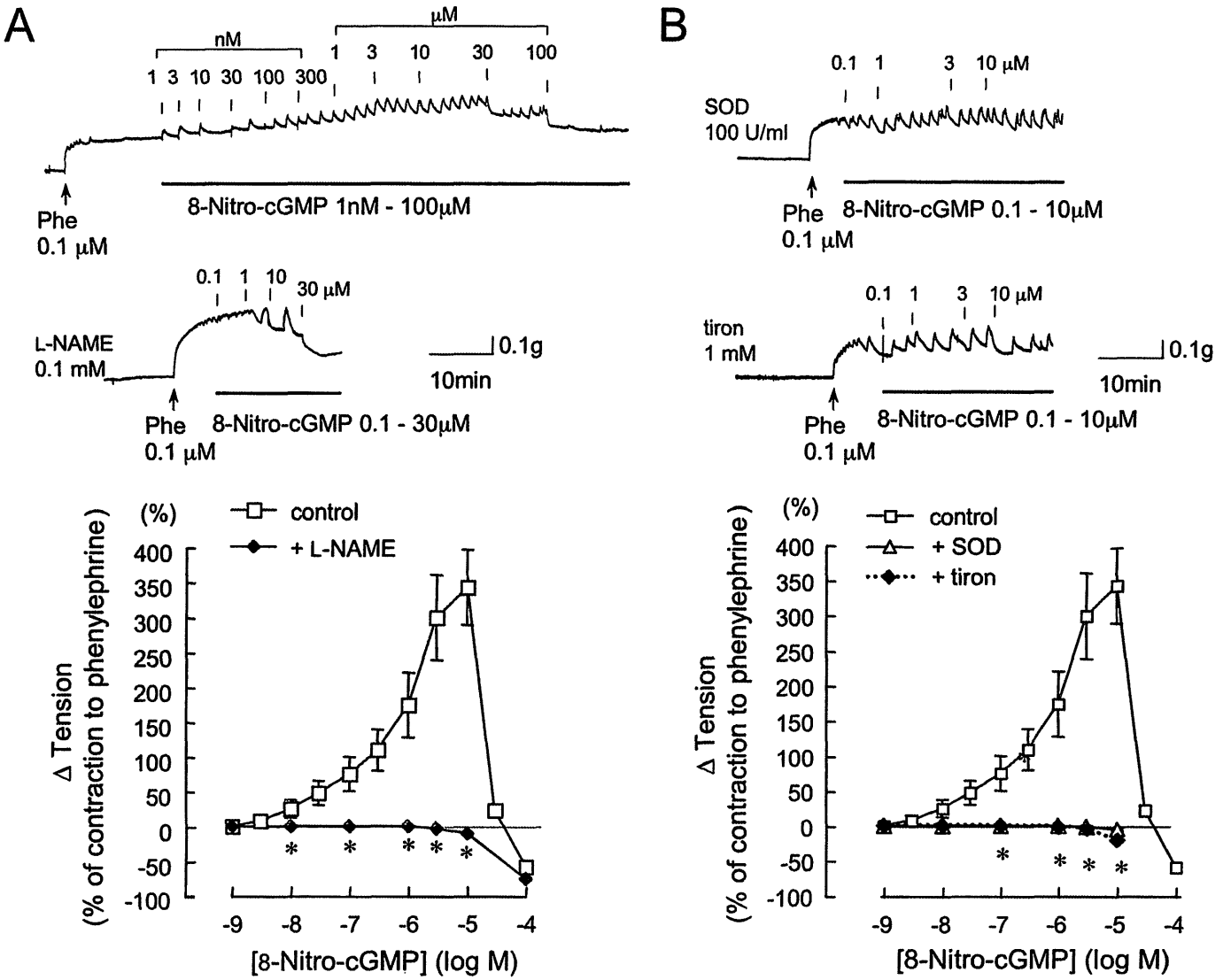

Figure 1

Effects of L-NAME, SOD and tiron on 8-nitro-cGMP-induced enhancement of contraction to phenylephrine (Phe) in aortic rings from C57BL/6 mouse. Original tracings and summarized data of vascular responses to cumulatively administered 8-nitro-cGMP in the Phe-contracted aorta. Vertical lines in each trace indicate administration of 8-nitro-cGMP. 8-Nitro-cGMP concentration-dependently produced a biphasic effect: an initial enhancement of contraction to Phe, followed by a relaxation. L-NAME (0.1 mM, A, lower trace), SOD (100 $U \cdot mL^{-1}$, B, upper trace) or tiron (1 mM, B, lower trace) was added 30 min before the addition of Phe (0.1 μM). L-NAME, SOD and tiron each abolished the enhancement of the contraction to Phe. Changes in vascular tension to 8-nitro-cGMP are expressed as % of the Phe-induced contraction. Each point represents the mean ± SEM ($n = 4$–6). *$P < 0.05$ versus control.

response to an exogenous NO donor, sodium nitroprusside, was not different in db/db and db/+ mice (data not shown).

Effects of 8-nitro-cGMP on Phe-induced contraction in diabetic mouse aorta

Typical responses of individual db/db and db/+ mouse aortas are shown in Figure 4A and B; the averaged concentration–response relationships from these experiments for both aortic rings are summarized in Figure 4C and D. In db/+ mice, the cumulative addition of 0.001–300 μM 8-nitro-cGMP produced a biphasic effect: at concentrations up to 10 μM the increase in tension of the Phe-contracted aortas was statistically significant, and at higher than 10 μM the contracted aortas were dose-dependently relaxed (Figure 4C). This enhancement of vasoconstriction by 8-nitro-cGMP was not observed in db/db mice, but only the relaxation was observed. The 8-bromo-cGMP-induced dose-dependent relaxation of the Phe-contracted rings was not significantly different in db/+ and db/db mice (Figure 4D). As shown in Figure 4A and B, 8-nitro-cGMP evoked a more rapid relaxant response than 8-bromo-cGMP in each mouse aorta.

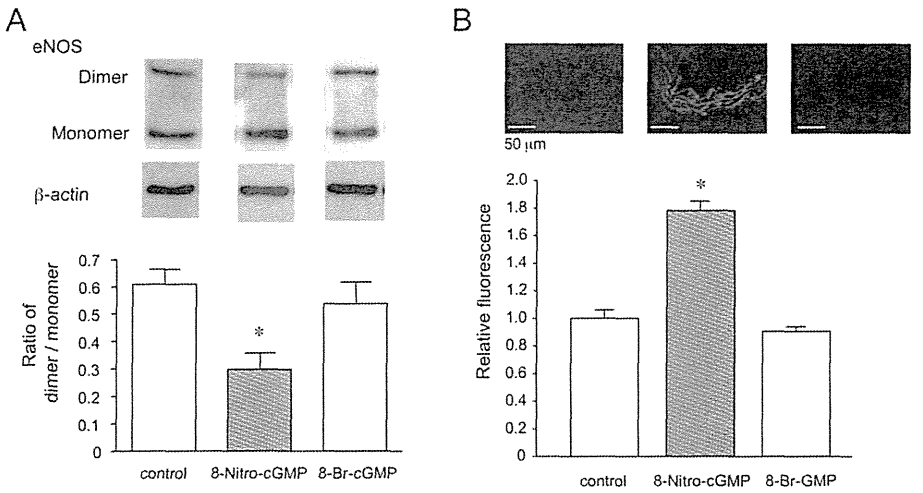

Figure 2

Disruption of eNOS dimer and superoxide production by 8-nitro-cGMP in aortas from C57BL/6 mouse. (A) Representative Western blots and densitometric analysis for eNOS dimer (280 KDa) and monomer (140 KDa) in C57BL/6 mouse aortic segments treated with vehicle, 8-nitro-cGMP or 8-bromo-cGMP. Each eNOS density was normalized to β-actin (45 KDa). (B) Representative fluorescent photomicrographs and quantitative analysis of DHE-labelled microscopic sections of C57BL/6 mouse aortic segments incubated with vehicle, 8-nitro-cGMP or 8-bromo-cGMP. Each value represents the mean ± SEM (n = 3–4). *P < 0.05 versus control and 8-bromo-cGMP.

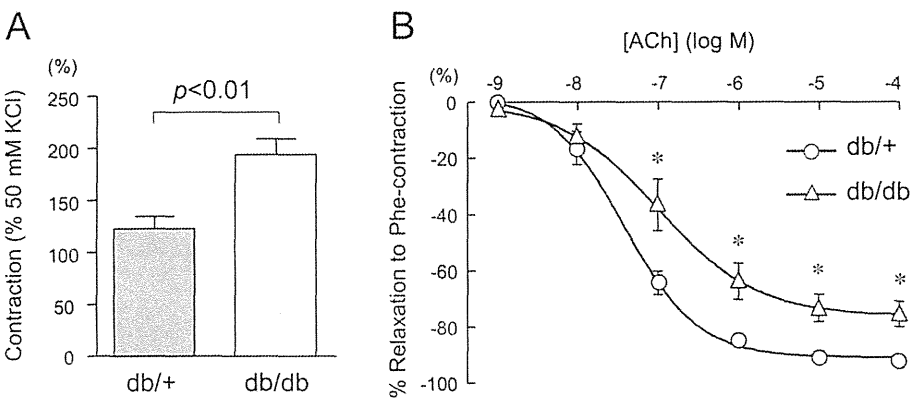

Figure 3

Vascular reactivity in aortas from db/+ and db/db mice. (A) Phe (0.1 μM)-induced contraction of thoracic aortic rings from db/+ and db/db mice. Data are expressed as % of the tension induced by 50 mM KCl. (B) Cumulative concentration–relaxation curves to acetylcholine (ACh) of Phe-contracted aortas from db/+ and db/db mice (n = 6 for each group). Relaxations are expressed as a percentage reversal of the contraction induced by Phe (1 μM). Data are shown as mean ± SEM. *P < 0.02 versus db/+.

Inhibitory effects of L-NAME *and a superoxide scavenger on 8-nitro-cGMP-induced enhancement of contraction to Phe in db/+ mouse aorta*

As shown in Figure 5, pretreatment of aortic rings from db/+ mouse with 100 μM L-NAME abolished the 8-nitro-cGMP-induced enhancement of the contraction to Phe. Moreover, in the presence of L-NAME, the vasorelaxant responses of 8-nitro-cGMP (300 μM) in db/+ aorta were stronger than those in the absence of L-NAME in db/db aorta (Figure 5A; db/+: −93.7 ± 0.01% tension, Figure 4C; db/db: −66.9 ± 4.3%, P < 0.05).

In agreement with the results with aortas from C57BL/6 mice, pretreatment of db/+ aortas with 100 U·mL^{-1} SOD abolished the 8-nitro-cGMP-induced enhancement of the contraction to Phe (Figure 5B). The potency of 1 mM tiron in aortas from db/+ mice was similar to that of SOD.

Indomethacin, a COX-1/2 inhibitor, did not affect the vascular responses elicited by 8-nitro-cGMP in both aortas from db/+ and db/db mice (data not shown). Moreover, L-NAME did not have a significant effect on the relaxation elicited by 8-nitro-cGMP in db/db aortas (data not shown).

Effects of a PDE5 inhibitor on 8-nitro-cGMP-induced relaxation of the contraction to Phe

A cGMP-specific PDE is responsible for degradation of cGMP in vascular tissues and thus the activity of PDE influences the

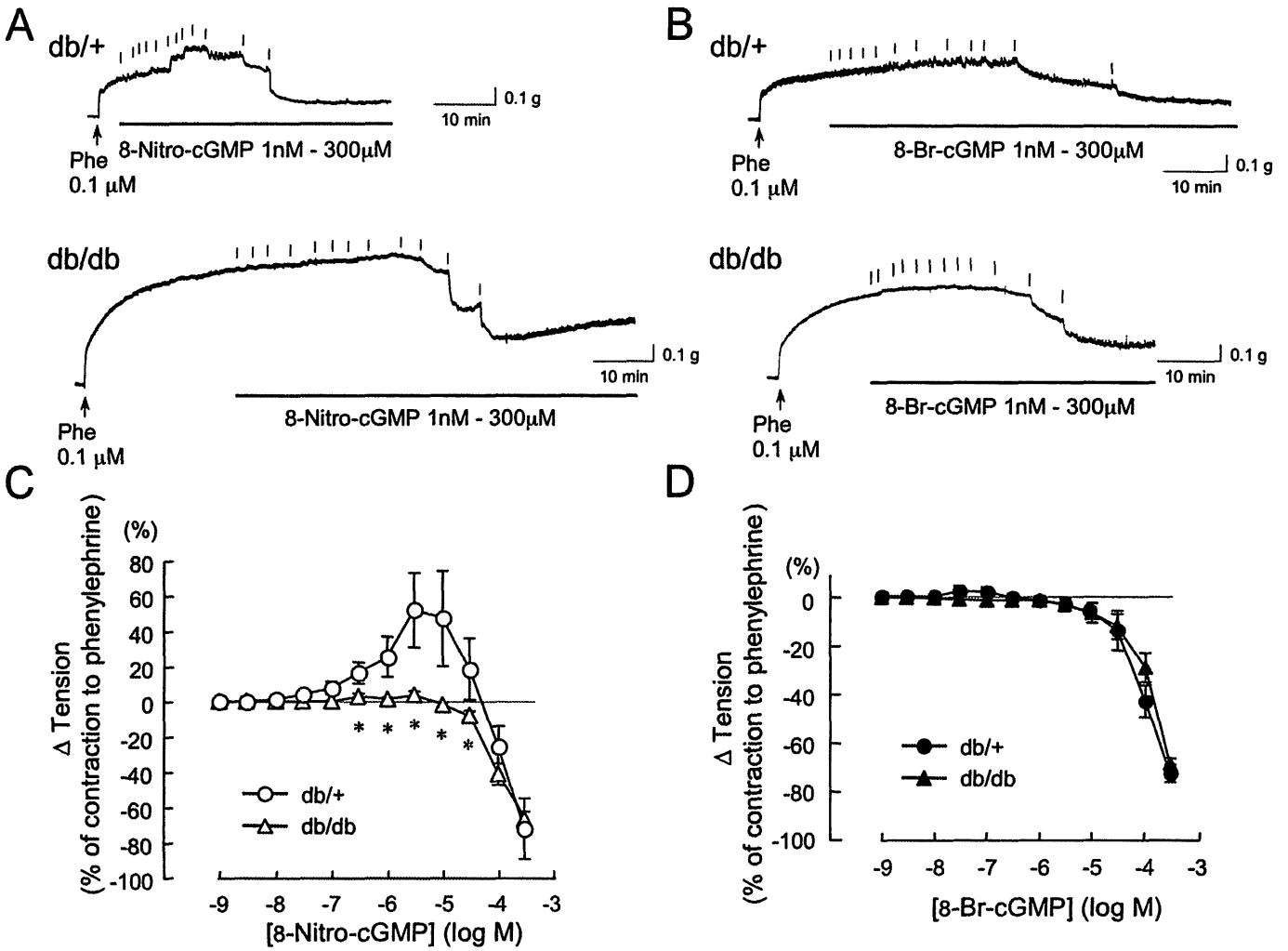

Figure 4

Effects of 8-nitro-cGMP on the contraction to Phe in the aortas from db/+ and db/db mice. Original tracings (A and B) and summarized data (C and D) of vascular responses to cumulatively administered 8-nitro-cGMP and 8-bromo-cGMP in the Phe-contracted aortas from db/+ and db/db mice. Vertical lines in each trace indicate administration of 8-nitro-cGMP (A) or 8-bromo-cGMP (B). Changes in vascular tension to 8-nitro-cGMP (C) and 8-bromo-cGMP (D) are expressed as % of the Phe (0.1 μM)-induced contraction. Each point represents the mean ± SEM (n = 5–9 for each group). *P < 0.05 versus db/+.

vascular tone. Pretreatment for 30 min with zaprinast (1 μM), a selective cyclic nucleotide PDE5 inhibitor, did not affect the concentration–response curve for 8-nitro-cGMP-induced relaxation in aortas from db/db mice (Figure 6A). In contrast, the vasorelaxant responses of 8-bromo-cGMP were enhanced in the presence of zaprinast (Figure 6B), indicating that 8-bromo-cGMP is probably degraded into inactive 5′-GMP. As shown in Figure 6C, the effect of 100 μM 8-bromo-cGMP was significantly enhanced by the zaprinast pretreatment.

Discussion

In the present study, we compared the effects of a novel nitrated derivative of cGMP, 8-nitro-cGMP, on vascular responses of aortas from non-diabetic and diabetic mice. Our data, showing that 8-nitro-cGMP induced enhancement of contraction to Phe and relaxation concentration-dependently in C57BL/6 and db/+ mice aortas (Figures 1A and 4A), are consistent with our previous study using normal rat carotid artery (Sawa *et al.*, 2007). In our previous study we also showed that the 8-nitro-cGMP-induced enhancement of vascular reactivity to Phe in the rat carotid artery is endothelium-dependent as removal of endothelium significantly attenuated the 8-nitro-cGMP-induced hyperreactivity. In addition, it was found that 8-nitro-cGMP caused no enhancement of contraction to Phe in aortas from eNOS-deficient mice. In the present study, we have demonstrated that pretreatment of C57BL/6 or db/+ aortas with L-NAME significantly reduces the 8-nitro-cGMP-induced enhancement of the contraction to Phe (Figures 1A and 5A), suggesting the involvement of eNOS in this hyperreactivity response. Furthermore, we showed, for the first time, that the 8-nitro-cGMP-induced enhancement of the contraction to

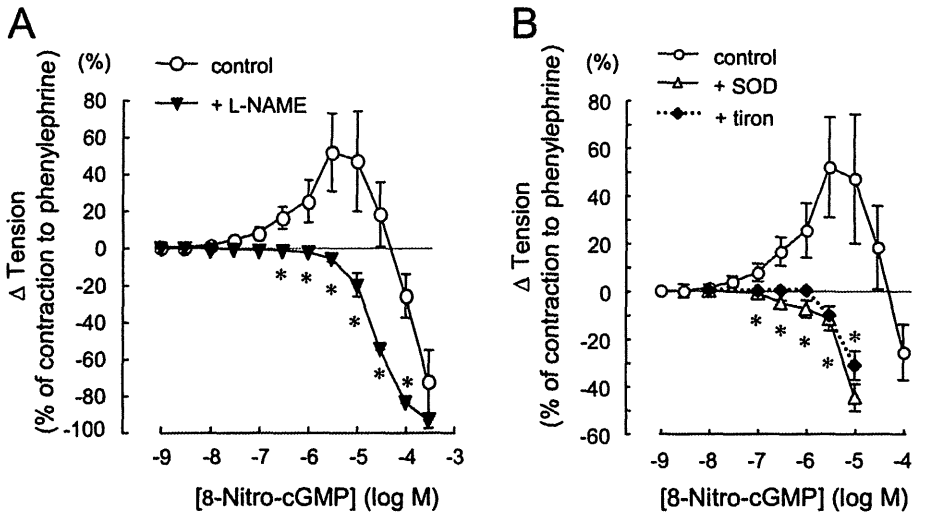

Figure 5

Effects of L-NAME, SOD and tiron on 8-nitro-cGMP-induced enhancement of the contraction to Phe in aortas from db/+ mice. L-NAME (0.1 mM, A), SOD (100 U·mL^{-1}, B) or tiron (1 mM, B) was added 30 min before the addition of Phe. Changes in vascular tension to 8-nitro-cGMP are expressed as % of the Phe-induced contraction in db/+ mouse aorta. Each point represents the mean ± SEM (n = 4–6). *P < 0.05 versus control.

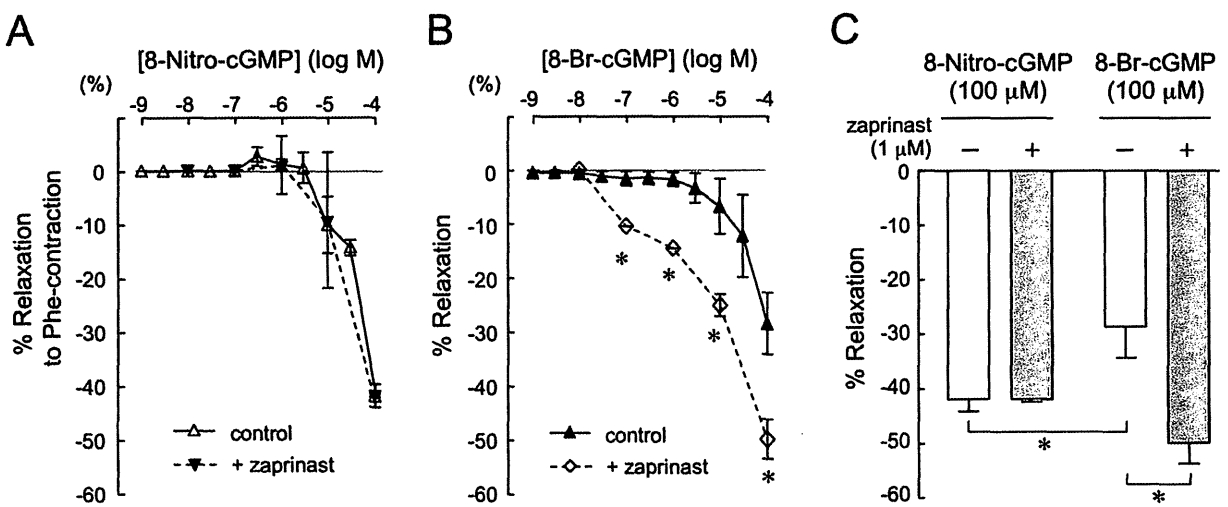

Figure 6

Effects of zaprinast on 8-nitro-cGMP or 8-bromo-cGMP-induced relaxation in db/db aorta contracted by Phe. Cumulative concentration–relaxation curves to 8-nitro-cGMP (A) or 8-bromo-cGMP (B) of the Phe-contracted aortas from db/db mice (n = 4–6 for each group). Zaprinast (1 μM) was added 30 min before the addition of Phe. (C) Comparison of the relaxation responses to 8-nitro-cGMP (100 μM) and 8-bromo-cGMP (100 μM) induced in the presence and absence of zaprinast in db/db aortic rings contracted by Phe. Data are shown as mean ± SEM. *P < 0.05 versus control.

Phe was not apparent in a db/db mouse aorta (Figure 4A), in which the contraction to Phe was enhanced (Figure 3A) and the endothelium-dependent relaxation to ACh was impaired (Figure 3B).

The spontaneously diabetic db/db mice used in the present study developed severe obesity, typically representing type 2 diabetes, which is associated with a substantially increased risk of cardiovascular disease. It has been demonstrated that Phe-induced contraction is enhanced and ACh-induced relaxation is inhibited in mesenteric artery from db/db mice, indicating impaired endothelial function (Pannirselvam *et al.*, 2002). Furthermore, Pannirselvam *et al.* (2003) have suggested that the cellular basis of endothelial dysfunction in the db/db mice may be due to an increased production of superoxide and decreased availability of tetrahydrobiopterin resulting in the uncoupling of eNOS. In the present study, using the db/db mouse aorta with increased vasocontractility to Phe, we observed that the 8-nitro-cGMP-induced enhancement of the contraction to Phe was absent in these aortas (Figure 4A and C). In contrast, vascular

responses to depolarization with KCl (50 mM) were similar in C57BL/6, db/+ and db/db mice aortas. Thus, it is unlikely that a generalized difference in vascular responsiveness or changes in calcium-activated contractile mechanisms are involved in the lack of an augmented Phe contractile response by 8-nitro-cGMP in db/db mice.

Furthermore we demonstrated, by use of Western blot analysis following low-temperature SDS-PAGE, that eNOS protein dimers can be disrupted, at least in part, by 8-nitro-cGMP in aortic segments from C57BL/6 mouse (Figure 2A). Additionally, an increase in superoxide production was detected in the 8-nitro-cGMP-treated aortic segments by use of DHE staining (Figure 2B). In contrast, 8-bromo-cGMP did not disrupt either the eNOS dimer or superoxide production in the C57BL/6 mouse aorta. These biological data support the idea that 8-nitro-cGMP may induce superoxide production via eNOS uncoupling. Thus, superoxide production by 8-nitro-cGMP may be involved in the enhancement of the Phe-induced contraction.

We have previously shown that NADPH oxidase-induced superoxide production in the db/db mice aortas is greater than those in db/+ mice (Dong *et al.*, 2010). It has also been suggested that eNOS exists in an uncoupled state and the nitrotyrosine level is higher in db/db mice aortas (Moien-Afshari *et al.*, 2008). Taken together, these results indicate that 8-nitro-cGMP does not enhance Phe-induced contractions in the db/db aortas because of a constitutively higher level of oxidative stress in these animals (Dong *et al.*, 2010) and uncoupled eNOS protein.

To determine the involvement of superoxide production in the 8-nitro-cGMP-induced enhancement of contraction to Phe, we tested the effects of the superoxide scavengers, SOD and tiron, on the 8-nitro-cGMP-induced enhancement of the contraction. Without contraction by Phe, 8-nitro-cGMP did not affect the basal tone of each aorta from non-diabetic and diabetic mice. We also found that SOD and tiron reduced the 8-nitro-cGMP-induced enhancement of contraction to Phe in C57BL/6 and db/+ mice aortas (Figures 1B and 5B), suggesting the involvement of superoxide.

As shown in Figure 3A, the contraction to Phe was enhanced in the vessels from db/db mice with endothelial dysfunction. We have also previously found that contraction to Phe is significantly enhanced in the aortas from eNOS-deficient mice and in the L-NAME-treated aortas from C57BL/6 mice, suggesting that eNOS is involved in the relaxation induced by α_1-adrenoceptor stimulation (Figure 7). Furthermore, in studies using α_1-blockers in rat aortas, it has been shown that NO can be released through stimulation of α_1-adrenoceptors on the endothelial cells and inhibits the contraction to noradrenaline (Kaneko and Sunano, 1993), and that α_1-adrenoceptors on the endothelial cells regulate angiogenesis (Ciccarelli *et al.*, 2008). As shown in Figure 7, an increase in intracellular Ca^{2+} via α_1-adrenoceptor stimulation, possibly in the endothelial cells, leads to activation of eNOS, which in turn may be uncoupled by the application of 8-nitro-cGMP and produce superoxide anion as we have previously suggested (Sawa *et al.*, 2007).

8-Nitro-cGMP not only enhanced the contraction to Phe in db/+ mouse aortas but also induced relaxation in Phe-contracted aortas from both db/+ and db/db mice (Figure 4A). Compared with 8-bromo-cGMP (100 μM)-induced relaxation, 8-nitro-cGMP (100 μM) induced a more rapid (Figure 4B) and larger (Figure 6C) relaxation response in the Phe-contracted aortas from C57BL/6, db/+ and db/db mice. In a previous study, by use of Western blot analysis, it was demonstrated that both 8-nitro-cGMP and 8-bromo-cGMP have strong protein kinase G (PKG)-activating potential, as shown by vasodilator-stimulated phosphoprotein phosphorylation in human uterine smooth muscle cells, which was inhibited by a PKG-specific inhibitor Rp-8-CPT-cGMPS [8-(4-chlorophenylthio)-guanosine 3′,5′-cyclic monophosphorothioate, Rp isomer] (Sawa *et al.*, 2007). Phosphorylation of several target proteins by PKG in vascular smooth muscle

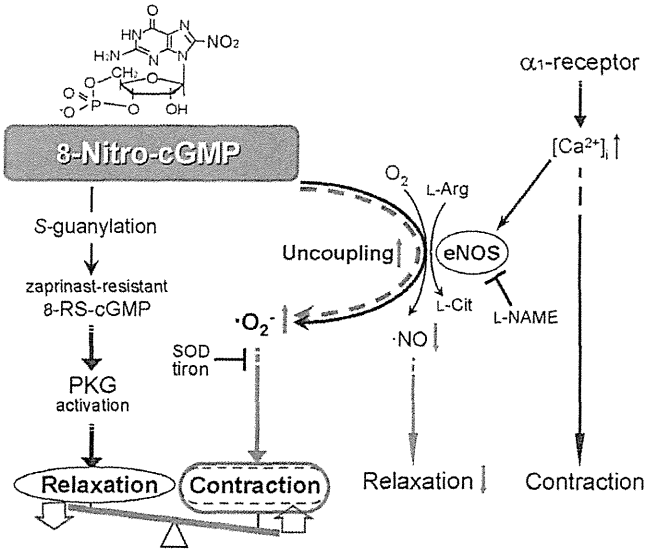

Figure 7

Hypothetical scheme for the mechanism that mediates the vascular tone induced by 8-nitro-cGMP. Stimulation of α_1-adrenoceptors by Phe increases intracellular Ca^{2+} concentrations ($[Ca^{2+}]_i$), leading to contraction of vascular smooth muscle cells. In vascular endothelial cells, concomitantly, eNOS is activated by the increase in $[Ca^{2+}]_i$ induced by α_1-adrenoceptor stimulation to produce NO and induce vascular relaxation via PKG activation. In the non-diabetic mouse aortas, 8-nitro-cGMP applied extracellularly may induce uncoupling (black line) of the eNOS activated by the Phe-induced increase in $[Ca^{2+}]_i$, and may produce superoxide ($\cdot O^{2-}$), resulting in enhancement of the Phe-induced contraction. In addition, not only PKG activation via 8-nitro-cGMP itself, but also 8-RS-cGMP, which is formed by protein S-guanylation and is resistant to PDE5, may induce a potentially strong PKG activation and then vasorelaxation. The rank order of potency for the effect of 8-nitro-cGMP at lower concentrations up to 10 μM is contraction > relaxation. However, the rank order reverses at higher concentrations of 8-nitro-cGMP. In the diabetic mouse aorta with eNOS uncoupling (red arrow), the relaxation via NO generation is depressed (red arrow) and superoxide is produced (red arrow), and thus the amplitude of the contraction induced by Phe is increased (red oval and seesaw-like balance). 8-Nitro-cGMP, applied in the diabetic aorta, does not induce eNOS uncoupling (broken blue line) and thus does not enhance Phe-contraction (blue oval), but induces only relaxation via PKG activation. The relaxant effect of 8-nitro-cGMP on the enhancement of vasoconstriction might be beneficial in compensating for excess oxidative stress (blue arrows), such as endothelial dysfunction of diabetic mice.

cells leads to a decrease in cytosolic Ca^{2+} and phosphorylated myosin, resulting in vascular relaxation (Lincoln and Cornwell, 1993; Feil *et al.*, 2003).

To address the potentially different relaxant effects of 8-nitro-cGMP and 8-bromo-cGMP, we compared their relaxation responses in the Phe-contracted aortas in the presence of a selective PDE5 inhibitor, zaprinast (Kukovetz *et al.*, 1979; Komas *et al.*, 1991; McMahon *et al.*, 1993). We observed that zaprinast significantly potentiated the relaxant effect of 8-bromo-cGMP, but not that of 8-nitro-cGMP, in the Phe-contracted aortas from db/db mouse, in which the 8-nitro-cGMP-induced enhancement of contraction to Phe was absent (Figure 6). Previously, it has been demonstrated that 8-nitro-cGMP reacts readily with the nucleophilic cysteine sulphhydryls (Cys-SH) of intracellular proteins and peptides, such as glutathione, to form adducts, 8-thioalkoxy-cGMP (8-RS-cGMP), via so-called S-guanylation (Figure 7) (Sawa *et al.*, 2003; 2007). Because 8-RS-cGMP may still have PKG activity and be resistant to the effects of PDE5, the relaxant response to 8-nitro-cGMP might be more resilient than that to 8-bromo-cGMP and not affected by the PDE5 inhibitor. Furthermore, in *in vitro* experiments with the recombinant PKG protein, we have found that PKG is highly sensitive to kinase activation by 8-nitro-cGMP (unpublished data). On the other hand, in our previous study we found that the membrane permeability of 8-nitro-cGMP in cultured cells is much less than that of 8-bromo-cGMP (Sawa *et al.*, 2007). Nevertheless, once 8-nitro-cGMP penetrates the cell membrane, intracellular 8-nitro-cGMP may have higher PKG activity than that of 8-bromo-cGMP for the reason described above.

Our data showing that 8-nitro-cGMP-induced relaxation in the Phe-contracted aorta from the non-diabetic mouse was enhanced in the presence of L-NAME (Figures 1A and 5A), are consistent with results from our previous study obtained in denuded rat carotid artery and eNOS-deficient mouse aorta (Sawa *et al.*, 2007). Recently, it was shown that superoxide production via eNOS uncoupling in rat aortic rings exposed to endothelin-1 is reduced by eNOS inhibition with L-NAME treatment and by endothelium denudation (Romero *et al.*, 2009). In our experiments with non-diabetic mice aortas (Figures 1A and 5A), inhibition of eNOS by L-NAME might lead to a reduction of superoxide generation via 8-nitro-cGMP-induced eNOS uncoupling, resulting in the suppression of 8-nitro-cGMP-induced contraction and thus an increase in relaxation. Whereas, in db/db mice aortas, with a constitutively high level of oxidative stress and eNOS protein in an uncoupled state (Moien-Afshari *et al.*, 2008; Dong *et al.*, 2010), as described above, 8-nitro-cGMP induced only a relaxation of the Phe-induced contraction, and L-NAME had no additive effect on the relaxation.

Furthermore, the 8-nitro-cGMP-induced relaxation was not inhibited by treatment with SOD or the non-catalytic tiron in the non-diabetic mice aortas (Figure 5B), but was decreased in the presence of a BK-type Ca^{2+}-activated K^+ channel blocker, iberiotoxin (100 nM), in the C57BL/6 mouse aortas. These results suggest the partial involvement of the BK-type Ca^{2+}-activated K^+ channels in the intracellular mechanism mediating relaxation; produced via 8-nitro-cGMP-induced activation of PKG.

Whether or to what extent changes in endogenous generation of 8-nitro-cGMP could contribute to impaired vascular reactivity in db/db mouse aorta still remain to be elucidated. Nevertheless, based on our present findings, 8-nitro-cGMP might be important not only in physiological functions but also in compensatory mechanisms for impaired vasodilatation induced by endothelial dysfunction, as depicted in Figure 7.

To summarize, we have demonstrated that 8-nitro-cGMP, applied acutely, induces bi-directional regulation of vascular responses, that is, enhancement of contraction and relaxation, in a dose-dependent manner in aortic rings from non-diabetic mice. In db/db mice with dysfunction of the vascular endothelial cells, only a vasorelaxation response that was resistant to a PDE5 inhibitor was induced by 8-nitro-cGMP. Therefore, the vasodilator effect of 8-nitro-cGMP might contribute to the amelioration of hypertension induced by vascular endothelial dysfunction, although further *in vivo* studies are needed to confirm this possibility. The effects of 8-nitro-cGMP might have important implications for therapeutic strategies aimed at restoring endothelial function.

Acknowledgements

This work was supported in part by Grants-in-Aid for scientific research from the Ministry of Education, Culture, Sports and Technology of Japan.

Conflict of interest

The authors have no conflicts of interest to declare.

References

Baynes JW, Thorpe SR (1999). Role of oxidative stress in diabetic complications: a new perspective on an old paradigm. Diabetes 48: 1–9.

Cai H, Harrison DG (2000). Endothelial dysfunction in cardiovascular diseases: the role of oxidant stress. Circ Res 87: 840–844.

Ciccarelli M, Santulli G, Campanile A, Galasso G, Cervèro P, Altobelli GG *et al.* (2008). Endothelial α_1-adrenoceptors regulate neo-angiogenesis. Br J Pharmacol 153: 936–946.

DeRubertis FR, Craven PA, Melhem MF, Salah EM (2004). Attenuation of renal injury in db/db mice overexpressing superoxide dismutase: evidence for reduced superoxide-nitric oxide interaction. Diabetes 53: 762–768.

Dong YF, Liu L, Kataoka K, Nakamura T, Fukuda M, Tokutomi Y *et al.* (2010). Aliskiren prevents cardiovascular complications and pancreatic injury in a mouse model of obesity and type 2 diabetes. Diabetologia 53: 180–191.

Feil R, Lohmann SM, de Jonge H, Walter U, Hofmann F (2003). Cyclic GMP-dependent protein kinases and the cardiovascular system: insights from genetically modified mice. Circ Res 93: 907–916.

Kaneko K, Sunano S (1993). Involvement of alpha-adrenoceptors in the endothelium-dependent depression of noradrenaline-induced contraction in rat aorta. Eur J Pharmacol 240: 195–200.

Komas N, Lugnier C, Stoclet JC (1991). Endothelium-dependent and independent relaxation of the rat aorta by cyclic nucleotide phosphodiesterase inhibitors. Br J Pharmacol 104: 495–503.

Kukovetz WR, Holzmann S, Wurm A, Poch G (1979). Evidence for cyclic GMP-mediated relaxant effects of nitro-compounds in coronary smooth muscle. Naunyn Schmiedebergs Arch Pharmacol 310: 129–138.

Lincoln TM, Cornwell TL (1993). Intracellular cyclic GMP receptor proteins. FASEB J 7: 328–338.

McMahon TJ, Ignarro LJ, Kadowitz PJ (1993). Influence of Zaprinast on vascular tone and vasodilator responses in the cat pulmonary vascular bed. J Appl Physiol 74: 1704–1711.

Mohazzab KM, Kaminski PM, Wolin MS (1994). NADH oxidoreductase is a major source of superoxide anion in bovine coronary artery endothelium. Am J Physiol 266: H2568–H2572.

Moien-Afshari F, Ghosh S, Elmi S, Rahman MM, Sallam N, Khazaei M *et al.* (2008). Exercise restores endothelial function independently of weight loss or hyperglycaemic status in db/db mice. Diabetologia 51: 1327–1337.

Nakamura T, Kataoka K, Fukuda M, Nako H, Tokutomi Y, Dong YF *et al.* (2009). Critical role of apoptosis signal-regulating kinase 1 in aldosterone/salt-induced cardiac inflammation and fibrosis. Hypertension 54: 544–551.

Pannirselvam M, Verma S, Anderson TJ, Triggle CR (2002). Cellular basis of endothelial dysfunction in small mesenteric arteries from spontaneously diabetic (db/db −/−) mice: role of decreased tetrahydrobiopterin bioavailability. Br J Pharmacol 136: 255–263.

Pannirselvam M, Simon V, Verma S, Anderson T, Triggle CR (2003). Chronic oral supplementation with sepiapterin prevents endothelial dysfunction and oxidative stress in small mesenteric arteries from diabetic (db/db) mice. Br J Pharmacol 140: 701–706.

Romero M, Jiménez R, Sánchez M, López-Sepúlveda R, Zarzuelo MJ, O'Valle F *et al.* (2009). Quercetin inhibits vascular superoxide production induced by endothelin-1: role of NADPH oxidase, uncoupled eNOS and PKC. Atherosclerosis 202: 58–67.

Sawa T, Akaike T, Ichimori K, Akuta T, Kaneko K, Nakayama H *et al.* (2003). Superoxide generation mediated by 8-nitroguanosine, a highly redox-active nucleic acid derivative. Biochem Biophys Res Commun 311: 300–306.

Sawa T, Zaki MH, Okamoto T, Akuta T, Tokutomi Y, Kim-Mitsuyama S *et al.* (2007). Protein S-guanylation by the biological signal 8-nitroguanosine 3′,5′-cyclic monophosphate. Nat Chem Biol 3: 727–735.

Vanhoutte PM, Shimokawa H, Tang EHC, Feletou M (2009). Endothelial dysfunction and vascular disease. Acta Physiol 196: 193–222.

Yamamoto E, Kataoka K, Shintaku H, Yamashita T, Tokutomi Y, Dong YF *et al.* (2007a). Novel mechanism and role of angiotensin II induced vascular endothelial injury in hypertensive diastolic heart failure. Arterioscler Thromb Vasc Biol 27: 2569–2575.

Yamamoto E, Yamashita T, Tanaka T, Kataoka K, Tokutomi Y, Lai ZF *et al.* (2007b). Pravastatin enhances beneficial effects of olmesartan on vascular injury of salt-sensitive hypertensive rats, via pleiotropic effects. Arterioscler Thromb Vasc Biol 27: 556–563.

Journal of Neurochemistry

JOURNAL OF NEUROCHEMISTRY | 2011 | 116 | 323–333

doi: 10.1111/j.1471-4159.2010.06916.x

Midbrain dopaminergic neurons utilize nitric oxide/cyclic GMP signaling to recruit ERK that links retinoic acid receptor stimulation to up-regulation of BDNF

Yuki Kurauchi,* Akinori Hisatsune,* Yoichiro Isohama,* Tomohiro Sawa,† Takaaki Akaike,† Koichi Shudo‡ and Hiroshi Katsuki*

*Department of Chemico-Pharmacological Sciences, Graduate School of Pharmaceutical Sciences, Kumamoto University, Kumamoto, Japan

†Department of Microbiology, Graduate School of Medical Sciences, Kumamoto University, Kumamoto, Japan

‡Research Foundation Itsuu Laboratory, Tokyo, Japan

Abstract

Stimulation of retinoic acid receptors (RARs) protects midbrain dopaminergic neurons, presumably via up-regulation of brain-derived neurotrophic factor (BDNF) expression. The present study was focused on unexplored signaling mechanisms linking RAR stimulation to BDNF expression. Rat midbrain slice cultures treated with an RAR agonist Am80 showed increased tissue levels of BDNF mRNA and protein as compared to cultures without treatment. Am80-induced increase in BDNF expression was observed in dopaminergic neurons, which was blocked by inhibition of extracellular signal-regulated kinase (ERK) activation. We also found that Am80 increased neuronal nitric oxide synthase expression in dopaminergic neurons even during ERK inhibition, and this increase was accompanied by 8-nitro-cyclic GMP formation. Notably, the effect of Am80 on BDNF expression was attenuated by inhibitors of nitric oxide synthase, soluble guanylyl cyclase and cyclic GMP-dependent protein kinase (PKG). Am80-induced ERK phosphorylation in dopaminergic neurons was also attenuated by inhibition of soluble guanylyl cyclase and PKG. Moreover, 8-Br-cyclic GMP induced ERK phosphorylation and BDNF expression in dopaminergic neurons. These results suggest that, by recruiting cyclic GMP and PKG, neuronal nitric oxide synthase-derived nitric oxide plays a novel and essential role in RAR signaling leading to ERK-dependent BDNF up-regulation in midbrain dopaminergic neurons.

Keywords: 8-nitro-cyclic GMP, neuronal nitric oxide synthase, neurotrophic factor, protein kinase G, retinoid, tamibarotene.

J. Neurochem. (2011) **116**, 323–333.

Retinoids have been originally defined as a group of natural and synthetic compounds that show biological activities similar to all-*trans*-retinoic acid (ATRA), a natural compound derived from vitamin A. Receptors mediating the actions of retinoids are designated as retinoic acid receptors (RARs) and retinoid X receptors (RXRs), both of which include α, β and γ subtypes (Maden 2007). These receptors comprise a part of nuclear receptor families. A classical mechanism of actions of retinoids involves formation of heterodimer between RAR and RXR, which is followed by binding of the heterodimer to retinoic acid-responsive element (RARE) located in the promoter region of various target genes (Maden 2007). On the other hand, RAR-mediated non-genomic mechanisms of signal transduction

Received April 24, 2010; revised manuscript received July 3, 2010; accepted July 13, 2010.

Address correspondence and reprint requests to Hiroshi Katsuki, Department of Chemico-Pharmacological Sciences, Graduate School of Pharmaceutical Sciences, Kumamoto University, 5-1 Oe-honmachi, Kumamoto 862-0973, Japan. E-mail: hkatsuki@gpo.kumamoto-u.ac.jp

Abbreviations used: AP-5, DL-2-amino-5-phosphono-pentanoic acid; ATRA, all-*trans*-retinoic acid; BDNF, brain-derived neurotrophic factor; ERK, extracellular signal-regulated kinase; GAPDH, glyceraldehyde-3-phosphate dehydrogenase; L-NAME, N^{ω}-nitro-L-arginine methyl ester; MEK, mitogen-activated protein kinase/ERK kinase; nNOS, neuronal nitric oxide synthase; ODQ, 1H-[1,2,4]oxadiazolo[4,3-*a*]quinoxalin-1-one; PI, phosphatidylinositide; PKG, cyclic GMP-dependent protein kinase; RAR, retinoic acid receptor; RARE, retinoic acid-responsive element; RXR, retinoid X receptor; TH, tyrosine hydroxylase; TrkB, tropomyosin-related kinase B.

that involves phosphatidylinositide (PI) 3-kinase and extracellular signal-regulated kinase (ERK) have also been reported (Cañón *et al.* 2004; Masiá *et al.* 2007; Chen and Napoli 2008).

Retinoid signaling plays a pivotal role in developmental processes of tissues and organs including CNS. However, RARs and RXRs are expressed also in many regions of adult CNS where mitosis and differentiation have been terminated (Zetterström *et al.* 1999; Gofflot *et al.* 2007), suggesting that they play distinct roles in adult CNS. In fact, accumulating evidence indicates that retinoid signaling may ameliorate several neuropathological conditions (Mey 2006; Malaspina and Michael-Titus 2008). For example, over-expression of RARβ promotes axon regeneration after spinal cord injury (Wong *et al.* 2006). Administration of ATRA ameliorates various neuropathological features and rescues spatial memory deficits in mouse model of Alzheimer disease (Ding *et al.* 2008; Shudo *et al.* 2009).

In a recent study, we examined the effect of Am80 (tamibarotene), a synthetic RARα/β agonist (Kagechika *et al.* 1988; Umemiya *et al.* 1997a), on inflammatory degeneration of midbrain dopaminergic neurons. We found that Am80 rescued dopaminergic neurons from degeneration induced by application of interferon-γ/lipopolysaccharide to organotypic midbrain slice cultures or by intranigral injection of lipopolysaccharide in mice *in vivo* (Katsuki *et al.* 2009). Results of detailed investigations *in vitro* suggested that the neuroprotective action of Am80 was mediated by brain-derived neurotrophic factor (BDNF). That is, Am80 induced phosphorylation of tropomyosin-related kinase B (TrkB), a high-affinity receptor for BDNF, in dopaminergic neurons, which was abolished by anti-BDNF neutralizing antibody. Moreover, the neuroprotective effect of Am80 was attenuated by anti-BDNF neutralizing antibody as well as a TrkB inhibitor. Acceleration of BDNF-mediated signaling by Am80 may be primarily attributable to an increase in BDNF expression, because Am80 up-regulated the expression of *bdnf* mRNA, but not of *trkB* mRNA (Katsuki *et al.* 2009).

Because the promoter region of *bdnf* gene does not contain putative RARE, up-regulation of BDNF expression by Am80 is unlikely to be mediated by direct regulation of *bdnf* transcription by classical retinoid signaling. Provided that BDNF plays important roles in brain physiology and pathophysiology (Hu and Russek 2008), the present study was aimed to reveal RAR-mediated signaling mechanisms leading to BDNF up-regulation.

Materials and methods

Culture preparation

Organotypic midbrain slice cultures were prepared according to the methods described previously (Katsuki *et al.* 2009; Kurauchi *et al.* 2009). All procedures were approved by animal experimentation committee of Kumamoto University, and were conformed to Basic Policy on Animal Experiments of The Ministry of Education, Culture, Sports, Science and Technology, Japan. Briefly, 2- to 3-day-old neonatal Wistar rats (Nihon SLC, Shizuoka, Japan) were anesthetized by hypothermia and decapitated, and the brain was removed from the skull and separated into two hemispheres. Coronal midbrain slices (350-μm thick) were prepared under sterile conditions with a tissue chopper, and transferred onto microporous membranes (Millicell-CM, Millipore, Bedford, MA, USA) in 6-well plates. Culture medium, consisting of 50% minimal essential medium/HEPES, 25% Hanks' balanced salt solution and 25% heat-inactivated horse serum (Invitrogen Japan, Tokyo, Japan) supplemented with 6.5 mg/mL glucose, 2 mM L-glutamine and 10 U/mL penicillin-G/10 μg/mL streptomycin, was supplied at a volume of 0.7 mL per each well. The culture medium was exchanged with fresh medium on the next day of culture preparation, and thereafter, every 2 days. Slices were maintained in a 34°C, 5% CO_2 humidified atmosphere.

Drug treatment

At 17 days *in vitro*, slices were incubated for 24 h in serum-free medium. Then slices were exposed to indicated concentrations of drugs by transfer of culture inserts to culture plates filled with 0.7 mL of drug-containing serum-free medium. Serum-free medium consisted of 75% minimal essential medium and 25% Hanks' balanced salt solution supplemented with 6.5 mg/mL glucose, 2 mM L-glutamine and 10 U/mL penicillin-G/10 μg/mL streptomycin. Drugs used were N^{ω}-nitro-L-arginine methyl ester (L-NAME; Sigma, St. Louis, MO, USA), *N*-[[3-(aminomethyl) phenyl]methyl]-ethanimidamide dihydrochloride (1400W; Tocris Cookson, Bristol, UK), 1H-[1,2,4]oxadiazolo[4,3-a]quinoxalin-1-one (ODQ; Wako, Osaka, Japan), 8-Br-cyclic GMP sodium salt (Biomol International, Plymouth Meeting, PA, USA), KT5823 (Wako), DL-2-amino-5-phosphono-pentanoic acid (AP-5; Sigma), (+)-MK801 hydrogen maleate (Sigma), PD98059 (Cayman Chemical, Ann Arbor, MI, USA), and LY294002 (Sigma). Am80, LE540 and HX630 were synthesized as described previously (Kagechika *et al.* 1988; Umemiya *et al.* 1997a,b).

Immunohistochemistry

Slices were fixed with 4% paraformaldehyde in 0.1 M phosphate buffer containing 4% sucrose at 4°C for 2.5 h, and double immunofluorescence was performed for combinations of tyrosine hydroxylase (TH) with BDNF, neuronal nitric oxide synthase (nNOS), 8-nitro-cyclic GMP or phosphorylated ERK. Mouse anti-TH (1 : 1000; Affinity BioReagents, Golden, CO, USA), rabbit anti-TH (1 : 1000; Millipore), rabbit anti-BDNF (1 : 200, sc-546; Santa Cruz Biotechnology, Santa Cruz, CA, USA), rabbit anti-nNOS (1 : 1000; Cell Signaling Tech., Danvers, MA, USA), mouse anti-8-nitro-cyclic GMP antibody (1 : 500; Sawa *et al.* 2007) and rabbit anti-phospho-ERK1/2 [phospho-p44/42 MAPK (Thr202/Tyr204), 1 : 1000; Cell Signaling Tech.] were used as primary antibodies. Alexa Fluor 488-conjugated goat anti-rabbit IgG(H + L) (1 : 500, Molecular Probes, Eugene, OR, USA) and Alexa Fluor 594-conjugated goat anti-mouse IgG(H + L) (1 : 500, Molecular Probes) were used as secondary antibodies. Fluorescence signals were observed with the use of a laser-scanning confocal microscope

system (Fluoview FV300, Olympus, Tokyo, Japan). Random fields of the substantia nigra in midbrain slices, identified by TH staining, were chosen blindly, and three or four fields in independent slices were examined in each set of experiments. Reproducibility of the results was confirmed by at least three independent sets of experiments.

Semi-quantitative RT-PCR

After treatment with drugs for 72 h, slices were collected in 1 mL of RNAiso Plus® reagent (TaKaRa, Shiga, Japan), homogenized on ice, and total RNA was extracted according to the manufacturer's instructions. RT-PCR was performed with an RNA PCR kit (AMV) Ver 3.0 (TaKaRa): 42°C for 60 min, 99°C for 5 min, and 5°C for 5 min for reverse transcription; 94°C for 30 s, 60°C for 30 s, and 72°C for 1 min for PCR [23 cycles for BDNF and 18 cycles for glyceraldehyde-3-phosphate dehydrogenase (GAPDH)]. PCR products were subjected to 2% agarose gel electrophoresis. Band intensities of ethidium bromide staining in the gels were analyzed with ImageJ software. The primer sequences were BDNF forward 5′-CCCAACGAAGAAAACCATAAG-3′, BDNF reverse 5′-CCCACTCGCTAATACTGTCAC-3′, GAPDH forward 5′-ACCATCTTCCAGGAGCGAGA-3′, GAPDH reverse 5′-CAGTCTTCTGGGTGGCAGTG-3′. GAPDH was used as an internal standard.

Real-time quantitative RT-PCR

Real-time PCR was performed with SYBR® Premix Ex Taq™ (TaKaRa) on a Chromo4™ real-time PCR analysis system (Bio-Rad, Tokyo, Japan). Samples were run in duplicate. The thermal cycling program consisted of 95°C for 3 min for polymerase activation, and then 40 cycles of denaturation (95°C for 15 s) and annealing and extension (60°C for 1 min). Reactions were quantified by selecting the amplification cycle when the PCR product of interest was first detected [the threshold cycle (Ct)]. Data were analyzed by the comparative Ct method. The primer sequences were the same as those listed above for semi-quantitative RT-PCR.

Western blotting

After treatment with Am80 for indicated periods, slices were collected in ristocetin-induced platelet agglutination buffer [150 mM NaCl, 50 mM Tris–HCl (pH 7.5), 5 mM EDTA, 1% Nonidet P-40 (Nacalai, Kyoto, Japan), 0.1% sodium dodecyl sulfate, 0.5% deoxycholate], and incubated at 4°C for 30 min. Lysates were centrifuged at 12 000 *g* at 4°C for 20 min and the protein concentration in each sample was determined by Bicinchoninate method. With added sample buffer containing 0.5 M Tris–HCl (pH 6.8), 10% sodium dodecyl sulfate, 2-mercaptoethanol, glycerol and 1% bromophenol blue, each sample was heated at 99°C for 10 min. Sodium dodecyl sulfate-polyacrylamide gel electrophoresis was performed on a 5.4% stacking gel with 15%, 8% or 12% separating gel for BDNF, nNOS or phospho-ERK, respectively. After gel electrophoresis, proteins were transferred onto polyvinylidene difluoride membranes. The blots were washed with Tris-buffered saline containing 0.1% Tween 20 and blocked with Blocking One (Nacalai) at 22–25°C for 2 h. The membrane was incubated with rabbit anti-BDNF antibody (1 : 1000), rabbit anti-nNOS antibody (1 : 1000), rabbit anti-phospho-ERK1/2 antibody [phospho-p44/42 MAPK (Thr202/Tyr204), 1 : 1000; Cell Signaling Tech.], rabbit anti-ERK antibody (p44/42 MAPK, 1 : 1000; Cell Signaling Tech.) and mouse anti-β-actin antibody (1 : 1000, Sigma) overnight at 4°C. After incubation with horseradish peroxidase-conjugated secondary antibodies at 22–25°C for 1 h, bands were detected with ECL Advance™ western blotting detection kit (Amersham Biosciences, Piscataway, NJ, USA) on a lumino-imaging analyzer (LAS-3000mini, Fuji Film, Tokyo, Japan).

Statistical analysis

Results are expressed as means ± SEM. Statistical significance of difference was evaluated with one-way ANOVA followed by Student-Newman-Keuls test, unless otherwise indicated. Probability values less than 5% were considered significant.

Results

RAR stimulation up-regulates BDNF expression in dopaminergic neurons

First, we examined the effect of RAR stimulation on BDNF protein levels in midbrain slice cultures, because the previous study addressed the level of *bdnf* mRNA only (Katsuki *et al.* 2009). Western blot analysis demonstrated that application of Am80 (300 nM) to midbrain slice cultures increased BDNF protein expression (Fig. 1a). The increase was evident at 48 h after initiation of Am80 treatment and was sustained for 72 h. The effect of Am80 on the levels of *bdnf* mRNA and BDNF protein was concentration-dependent in a range between 30 and 300 nM (Fig. 1b and c). As reported previously (Katsuki *et al.* 2006), dopaminergic neurons comprise less than 3% of all neurons within midbrain slice cultures under the present experimental conditions. Therefore, the levels of expression of BDNF in whole tissues determined as above do not provide adequate information concerning BDNF expression in dopaminergic neurons. To examine whether the increase in BDNF expression occurred in dopaminergic neurons, we carried out double immunofluorescence staining against BDNF and TH. Although several TH-immunoreactive dopaminergic neurons exhibited BDNF immunoreactivity even under control conditions without treatment, BDNF immunoreactivity was markedly increased in dopaminergic neurons as well as in other cells surrounding dopaminergic neurons, after treatment with 300 nM Am80 for 72 h (Fig. 1d).

Am80 shows agonistic activity on RARα and RARβ, but not on RXRs (Umemiya *et al.* 1997a). Indeed, both semi-quantitative RT-PCR analysis and western blot analysis demonstrated that concomitant application of an RAR antagonist LE540 (1 μM) for 72 h prevented the increase in *bdnf* mRNA and BDNF protein expression induced by Am80 (data not shown). On the other hand, an RXR agonist HX630 (1 μM) did not affect BDNF expression. Similarly, Am80-induced up-regulation of BDNF immunoreactivity in dopaminergic neurons was reduced by LE540 but was not influenced by HX630 (Fig. 1d).

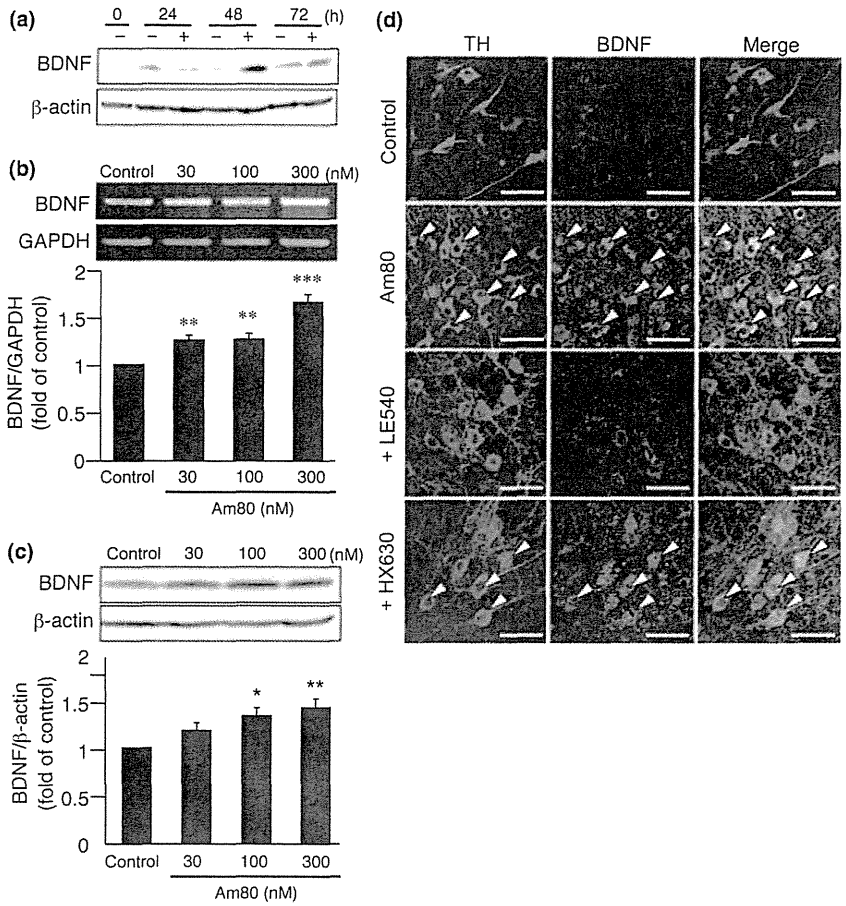

Fig. 1 RAR stimulation increases BDNF expression in dopaminergic neurons. (a) Western blot analysis of the effect of an RAR agonist Am80 on expression levels of BDNF protein. Midbrain slice cultures were treated with 300 nM Am80 for indicated periods. Six slices for each condition were pooled for each lane. (b) Semi-quantitative RT-PCR analysis of *bdnf* mRNA expression, showing the effect of Am80 applied at indicated concentrations for 72 h. $n = 6$. $^{**}p < 0.01$, $^{***}p < 0.001$ vs. control. (c) Western blot analysis of BDNF protein levels after 72-h treatment with indicated concentrations of Am80. $n = 6$. $^{*}p < 0.05$, $^{**}p < 0.01$ vs. control. (d) Double immunofluorescence histochemistry on TH (left panels) and BDNF (middle panels), and merged images (right panels) after 72-h treatment with 300 nM Am80. An RAR antagonist LE540 (1 μM) and an RXR agonist HX630 (1 μM) were applied concomitantly with Am80. Representative TH-positive cells with intense BDNF immunoreactivity are indicated by arrowheads. Scale bars, 50 μm.

ERK mediates up-regulation of BDNF expression by RAR stimulation

Mitogen-activated protein kinase/ERK kinase (MEK)/ERK signaling pathway has been reported to mediate regulation of BDNF expression in many neuronal cell types (Greer and Greenberg 2008). In addition, we and others have shown that RAR stimulation can recruit MEK/ERK signaling (Cañón *et al.* 2004; Chen and Napoli 2008; Katsuki *et al.* 2009). Accordingly, we examined the effect of PD98059, a MEK1 inhibitor, on Am80-induced increase in BDNF expression. Semi-quantitative RT-PCR demonstrated that concomitant application of PD98059 (20 μM) for 72 h prevented the increase in *bdnf* mRNA expression by Am80 (Fig. 2a). The effect of PD98059 against *bdnf* mRNA up-regulation was confirmed by real-time quantitative RT-PCR (Figure S1). We also examined the effect of LY294002, a PI3-kinase inhibitor, because LY294002 blocks neuroprotective effect of Am80 on dopaminergic neurons (Katsuki *et al.* 2009). LY294002 (50 μM) did not prevent the increase in *bdnf* mRNA (Fig. 2a). Consistent results were obtained from western blot analysis (data not shown) and immunohistochemical examinations, where PD98059 reduced BDNF up-regulation in dopaminergic neurons induced by Am80 (Fig. 2b).

RAR stimulation up-regulates nNOS expression and triggers NO-related signaling

Nitric oxide plays an important role in intra- and intercellular signaling in CNS (Calabrese *et al.* 2007). During the course of investigation, we found that NO-related signal transduction pathway was involved in RAR signaling. In control cultures, nNOS immunoreactivity was mainly local-

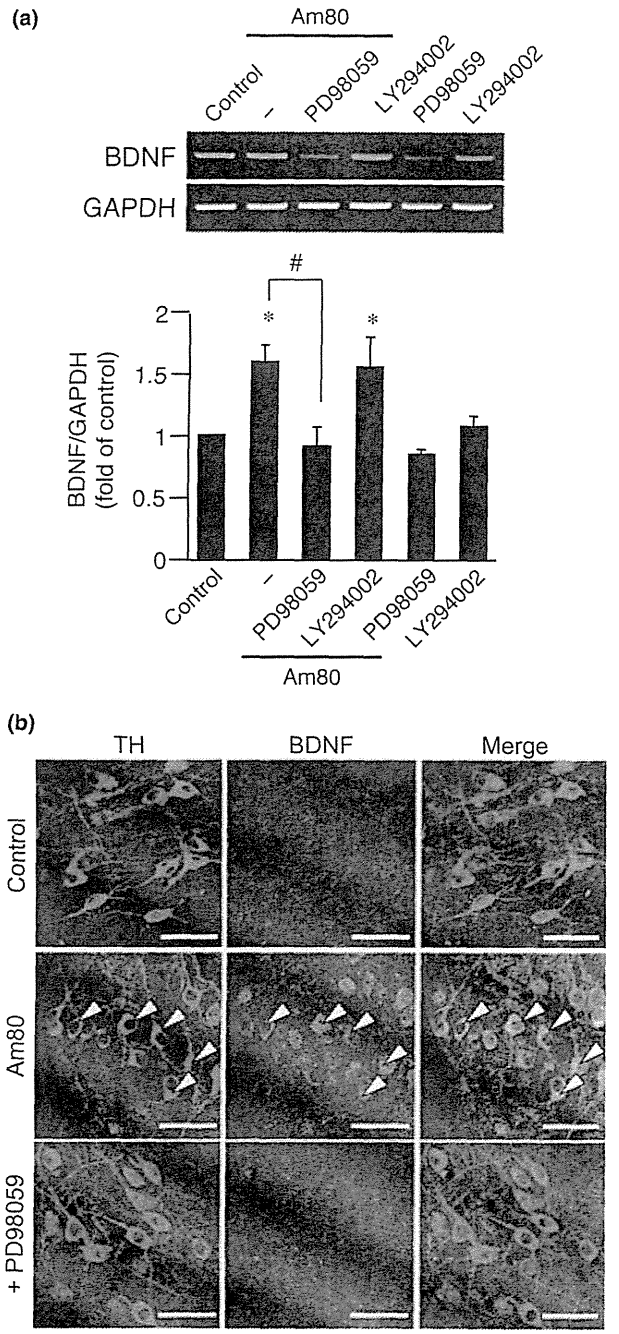

Fig. 2 RAR stimulation increases BDNF expression in dopaminergic neurons via MEK/ERK but not PI3-kinase signaling pathway. (a) Effect of a MEK1 inhibitor, PD98059 (20 μM), and a PI3-kinase inhibitor, LY294002 (50 μM), on *bdnf* mRNA expression induced by 72-h treatment with 300 nM Am80. $n = 5$. $^{*}p < 0.05$ vs. control; $\#p < 0.05$. (b) Double immunofluorescence histochemistry on TH (*left panels*) and BDNF (middle panels), and merged images (right panels) after 72-h treatment with 300 nM Am80. PD98059 (20 μM) was applied concomitantly with Am80. Representative TH-positive cells with intense BDNF immunoreactivity are indicated by arrowheads. Scale bars, 50 μm.

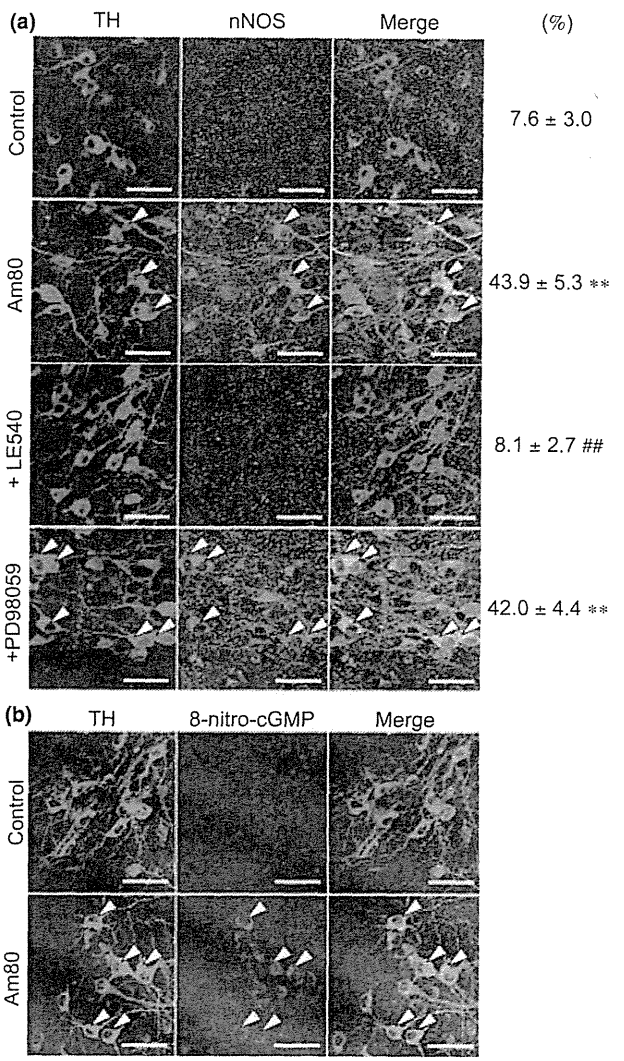

Fig. 3 RAR stimulation increases nNOS expression and activates NO/cyclic GMP signaling in dopaminergic neurons. (a) Confocal images of double immunofluorescence histochemistry on TH (left panels) and nNOS (middle panels), and merged images (right panels) after 24-h treatment with 300 nM Am80. LE540 (1 μM) and PD98059 (20 μM) were applied concomitantly with Am80. Doubly positive cells are indicated by arrowheads. Values given on the right represent the percentage of TH-positive cells showing nNOS immunoreactivity ($n = 6$ for each condition). $^{**}p < 0.01$ compared with control; $\#\#p < 0.01$ compared with Am80 alone. (b) Confocal images of double immunofluorescence histochemistry on TH (left panels) and 8-nitro-cyclic GMP (middle panels), and their merged images (right panels) after 24-h treatment with 300 nM Am80. Doubly positive cells are indicated by arrowheads. Scale bars, 50 μm.

ized in midbrain cells other than dopaminergic neurons. In contrast, we observed intense nNOS immunoreactivity in several dopaminergic neurons as early as 24 h after application of Am80 (Fig. 3a), and the intense immunoreactivity was sustained at 72 h. Increase in nNOS immunoreactivity in response to Am80 was observed also in putative neuronal cells other than dopaminergic neurons. Up-regulation of

nNOS protein by 24-h treatment with Am80 was confirmed by western blot analysis (Figure S2a). Concomitant application of an RAR antagonist LE540 (1 μM) for 24 h prevented the increase in nNOS immunoreactivity in dopaminergic neurons by Am80, as assessed by the percentage of TH-positive cells expressing nNOS. Notably, a MEK1 inhibitor PD98059 (20 μM) did not affect nNOS expression induced by Am80 (Fig. 3a).

To verify if up-regulated nNOS correspondingly recruited its downstream signaling, we examined production of 8-nitro-cyclic GMP. 8-Nitro-cyclic GMP is a recently identified signaling molecule that is generated by nitration of cyclic GMP (Sawa *et al.* 2007). As NO activates soluble guanylyl cyclase that mediates formation of cyclic GMP, generation of 8-nitro-cyclic GMP provides evidence for mobilization of NO/soluble guanylyl cyclase/cyclic GMP signaling. Immunohistochemical examination revealed that 24-h treatment with 300 nM Am80 increased 8-nitro-cyclic GMP immunoreactivity in dopaminergic neurons as well as in other cells (Fig. 3b).

NO/cyclic GMP/protein kinase G signaling mediates BDNF up-regulation by RAR stimulation

The above results indicate that RARs recruit NO/cyclic GMP signal in dopaminergic neurons. To clarify if this signaling pathway was involved in up-regulation of BDNF expression, we examined effects of several drugs interfering NO/cyclic GMP signal. Semi-quantitative RT-PCR showed that a general NOS inhibitor L-NAME (1 mM) prevented the increase in *bdnf* mRNA expression induced by 72-h treatment with 300 nM Am80. On the other hand, an inducible NOS-selective inhibitor 1400W (100 μM) did not prevent *bdnf* mRNA expression (Fig. 4a). Am80-induced expression of *bdnf* mRNA was also suppressed by ODQ (100 μM), a soluble guanylyl cyclase inhibitor, or by KT5823 (10 μM), a cyclic GMP-dependent protein kinase (PKG) inhibitor (Fig. 4b). Abrogation by L-NAME and ODQ of the effect of Am80 on *bdnf* mRNA expression was also confirmed by real-time quantitative RT-PCR (Figure S1). We obtained essentially the same results by western blot analysis on BDNF protein, with regard to the effect of L-NAME, 1400W, ODQ and KT5823 (data not shown). In agreement with these results, Am80-induced increase in BDNF immunoreactivity in TH-positive dopaminergic neurons was reduced by L-NAME and ODQ, but not by 1400W (Fig. 4c). Moreover, 72-h application of 8-Br-cyclic GMP (100 μM), a membrane-permeable cyclic GMP analog, increased *bdnf* mRNA expression by 44.4 ± 3.0% ($n = 6$, $p < 0.05$ vs. control by Wilcoxon matched-pairs signed-ranks test) and BDNF immunoreactivity in dopaminergic neurons (Fig. 4c).

NO/cyclic GMP/PKG signaling mediates ERK activation by RAR stimulation

So far, we demonstrated that both MEK/ERK signaling pathway and NO/cyclic GMP/PKG signaling pathway are involved in BDNF up-regulation by Am80. Because nNOS expression by Am80 was not blocked by PD98059 (Fig. 3a), MEK/ERK is unlikely to act upstream of NO/cyclic GMP/PKG signaling pathway. Therefore, we examined whether ERK acted downstream of NO signaling, by double immunofluorescence staining against TH and phosphorylated ERK1/2 (Fig. 5). Under control conditions, phosphorylated ERK1/2 was detected mainly in cells other than dopaminergic neurons. By contrast, we observed increased phosphorylation of ERK1/2 prominently in dopaminergic neurons at 24 h after application of Am80, which was consistent with our previous finding (Katsuki *et al.* 2009). Increased phosphorylation of ERK1/2 by 24-h treatment with Am80 was also confirmed by western blot analysis (Figure S2b). The increase in phosphorylated ERK1/2 was prevented by an RAR antagonist LE540: the percentage of TH-positive cells with phosphorylated ERK was 44.2 ± 7.0% ($n = 6$) and 9.7 ± 3.4% ($n = 6$), in slices treated for 24 h with 300 nM Am80 alone and those treated with 300 nM Am80 plus 1 μM LE540, respectively ($p < 0.05$). Moreover, concomitant application of ODQ (100 μM) or KT5823 (10 μM) for 24 h also prevented the increase in phosphorylated ERK1/2 induced by Am80. Conversely, 24-h application of 8-Br-cyclic GMP (100 μM) alone increased dopaminergic neurons positive for phosphorylated ERK1/2 (Fig. 5). These results suggest that MEK/ERK signaling pathway acts downstream of NO/cyclic GMP/PKG signaling to increase BDNF expression in dopaminergic neurons.

NMDA receptors are involved in BDNF up-regulation by RAR stimulation

Neuronal nitric oxide synthase, a Ca^{2+}/calmodulin-dependent enzyme, is known to associate with NMDA subtype of glutamate receptors that constitutes an important Ca^{2+} entry site in neurons (Esplugues 2002). Accordingly, we examined the effect of NMDA receptor antagonists on NO signaling and BDNF expression induced by Am80. Concomitant application of AP-5 (50 μM), a competitive NMDA receptor antagonist, or MK-801 (10 μM), an NMDA receptor channel blocker, for 72 h prevented the increase in BDNF expression by Am80 (Fig. 6a). Both AP-5 (data not shown) and MK-801 also inhibited up-regulation of BDNF immunoreactivity by Am80 in dopaminergic neurons (Fig. 6b). We also found that AP-5 and MK-801 inhibited production of 8-nitro-cyclic GMP induced by Am80 (data not shown). In contrast, appearance of intense nNOS immunoreactivity after 24 h of Am80 treatment was not prevented by AP-5 or MK-801 (Fig. 6c). The percentage of TH-positive cells expressing nNOS was 45.1 ± 6.9% ($n = 6$) and 42.0 ± 5.8% ($n = 6$), in slices treated for 24 h with 300 nM Am80 plus 50 μM AP-5 and those treated with 300 nM Am80 plus 10 μM MK-801, respectively. These values were not significantly different from the value in slices treated with Am80 alone (43.9 ± 5.3%, $n = 6$).

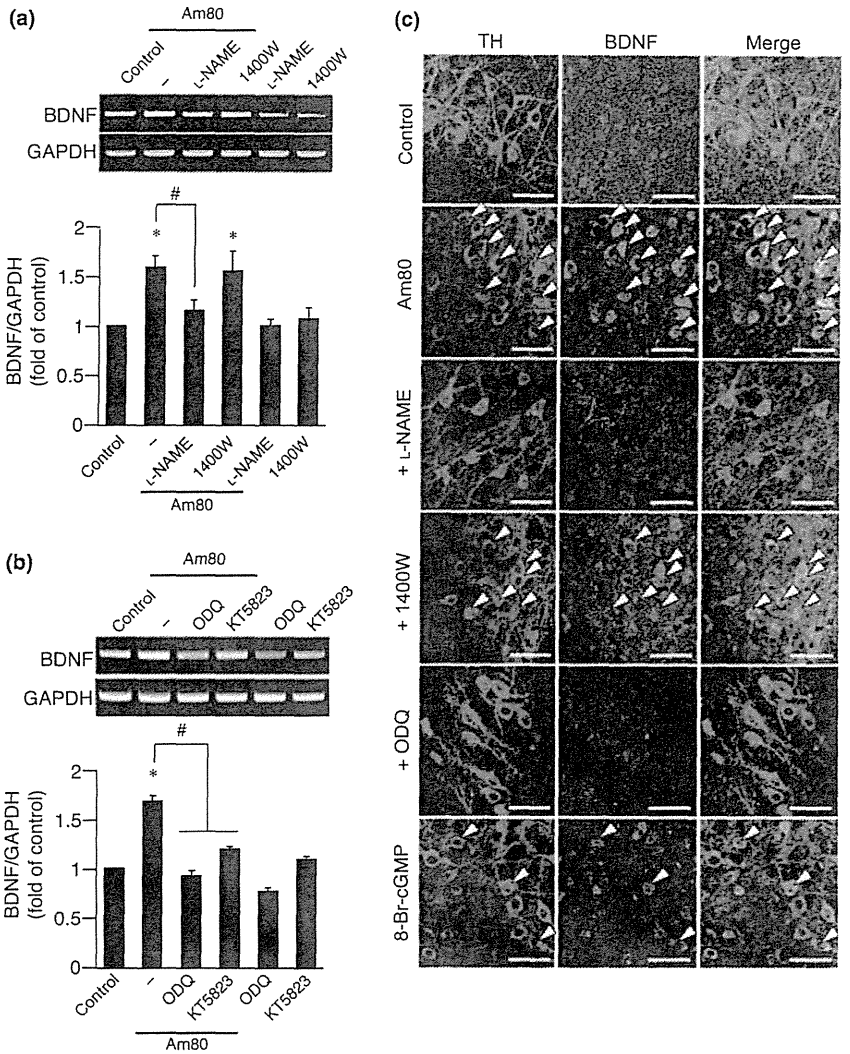

Fig. 4 RAR stimulation increases BDNF expression in dopaminergic neurons via NO/cyclic GMP/PKG signaling pathway. (a) Effects of L-NAME (1 mM) and 1400W (100 μM) on *bdnf* mRNA expression induced by 72-h treatment with 300 nM Am80. $n = 5$. $^*p < 0.05$ vs. control; $\#p < 0.05$. (b) Effects of ODQ (100 μM) and KT5823 (10 μM) on *bdnf* mRNA expression induced by 72-h treatment with 300 nM Am80. $n = 5$. $^*p < 0.05$ vs. control; $\#p < 0.05$. (c) Double immunofluorescence histochemistry on TH (left panels) and BDNF (middle panels), and merged images (right panels) after 72-h treatment with 300 nM Am80 or 100 μM 8-Br-cyclic GMP. L-NAME (1 mM), 1400W (100 μM) and ODQ (100 μM) were applied concomitantly with Am80. Representative TH-positive cells with intense BDNF immunoreactivity are indicated by arrowheads. Scale bars, 50 μm.

Discussion

Brain-derived neurotrophic factor is one of the key signaling molecules that maintain survival of neurons in normal and diseased CNS (Hu and Russek 2008). Our previous study reported that the neuroprotective action of an RAR agonist Am80 on midbrain dopaminergic neurons was mediated by up-regulation of BDNF (Katsuki *et al.* 2009). Accordingly, here we examined the mechanisms of BDNF up-regulation by RARs in midbrain slice culture. We found that nNOS induction linked RAR stimulation to BDNF up-regulation, via cyclic GMP/PKG signaling and ERK activation (Figure S3).

We showed previously that *bdnf* mRNA expression was increased by Am80 treatment (Katsuki *et al.* 2009). In the present study we confirmed that BDNF increased also at protein levels in response to Am80. Immunohistochemical localization demonstrated that dopaminergic neurons as well as surrounding cells express BDNF, suggesting that BDNF can exert neuroprotective and neurotrophic effects on dopaminergic neurons in an autocrine/paracrine manner. The effect of Am80 was blocked by an RAR antagonist LE540, indicating that RARs mediated up-regulation of BDNF by Am80.

In many cell types, expression of BDNF is under control of ERK, because ERK phosphorylates and activates a

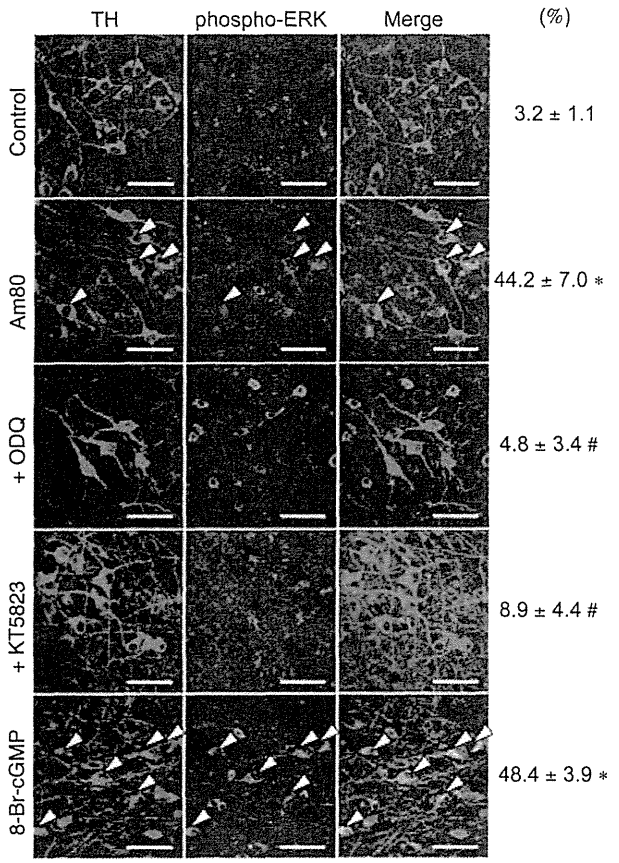

Fig. 5 NO/cyclic GMP signaling mediates ERK activation following RAR stimulation in dopaminergic neurons. Shown are confocal images of double immunofluorescence histochemistry on TH (left panels) and phosphorylated ERK1/2 (middle panels), and their merged images (right panels) after 24-h treatment with 300 nM Am80 or 100 μM 8-Br-cyclic GMP. ODQ (100 μM) and KT5823 (10 μM) were applied concomitantly with Am80. Doubly positive cells are indicated by arrowheads. Scale bars, 50 μm. Values given on the right represent the percentage of TH-positive cells with phosphorylated ERK ($n = 6$ for each condition). *$p < 0.05$ compared with control; #$p < 0.05$ compared with Am80 alone, by non-parametric Kruskal–Wallis test followed by Dunn's multiple range test.

transcription factor cyclic AMP-response element binding protein that directly binds to *bdnf* promoter to induce gene transcription (Greer and Greenberg 2008). Consistent with this notion, we found that BDNF up-regulation by Am80 was prevented by PD98059. On the other hand, PI3-kinase inhibitor LY294002 showed no effect on BDNF expression, although this drug, as well as PD98059, has been shown to block the neuroprotective effect of Am80 (Katsuki *et al.* 2009). Hence, PI3-kinase may act downstream of ERK-mediated BDNF expression in Am80-induced dopaminergic neuroprotection. These results indicate that RAR signaling in the midbrain differs from that in SH-SY5Y neuroblastoma cells where non-genomic recruitment of PI3-kinase occurs in response to RAR activation (Masiá *et al.* 2007), and also from that in striatal medium spiny neurons where ATRA recruits PI3-kinase (Pedrini *et al.* 2008).

A notable finding was that Am80 increased nNOS expression in midbrain slice culture via RAR stimulation. Retinoid-induced expression of nNOS in mature neurons was an unprecedented finding, although in some cases ATRA increases nNOS expression or NO production concomitantly with differentiation of neuroblastoma cell lines (Ghigo *et al.* 1998; Personett *et al.* 2000). Increased nNOS expression was expected to recruit cyclic GMP signaling, as NO activates soluble guanylyl cyclase. Activation of NO/cyclic GMP signaling by Am80 treatment was confirmed by increased production of 8-nitro-cyclic GMP, a recently identified molecule involved in intracellular signaling. 8-Nitro-cyclic GMP may exert biological actions via several mechanisms, one of which is activation of PKG as a stable analog of cyclic GMP (Sawa *et al.* 2007). Am80-induced up-regulation of BDNF was prevented by inhibition of NOS, soluble guanylyl cyclase and PKG, indicating that NO/cyclic GMP/PKG signals mediate the action of Am80 on BDNF expression. Detailed mechanisms of the increase in nNOS expression remain to be determined. As RARE-mediated regulation has not been reported for nNOS expression, one may assume indirect regulation of gene expression by RAR-mediated non-genomic signal transduction mechanisms involving PI3-kinase or ERK (Cañón *et al.* 2004; Masiá *et al.* 2007; Chen and Napoli 2008). However, although ATRA has been recently reported to induce nNOS expression in human neuroblastoma cells in a PI3-kinase-dependent manner (Nagl *et al.* 2009), nNOS expression induced by Am80 in our preparation was not blocked by a PI3-kinase inhibitor. We also observed that PD98059 showed no effect on nNOS up-regulation, indicating that ERK does not act upstream of NO signaling. This observation contrasts with reports from other groups showing that ERK1/2 is promptly recruited in response to ATRA in PC12 subclones and cultured hippocampal neurons (Cañón *et al.* 2004; Chen and Napoli 2008). Notably, a recent study reported a novel RXR- and RARE-independent regulatory mechanism of gene transcription by RAR, where complex of RAR with a transcription factor neurogenin2 recruits histone acetyltransferase, cyclic AMP-response element binding protein-binding protein, to motor neuron enhancers, resulting in motoneuron gene expression (Lee *et al.* 2009).

Pharmacological examinations on phospho-ERK levels in Am80-treated slice cultures demonstrated that cyclic GMP/PKG signals act upstream of ERK activation. That is, Am80-induced increase in phospho-ERK immunoreactivity was blocked by inhibition of soluble guanylyl cyclase and PKG, and 8-Br-cyclic GMP could increase phospho-ERK in dopaminergic neurons. Mechanisms of ERK activation by NO/cyclic GMP/PKG pathway remain unclear, but NO/cyclic GMP/PKG-dependent ERK activation has been reported in the lateral amygdala during memory consolidation (Ota *et al.* 2008). In the avian retina, NO-dependent

ERK activation is mediated by soluble guanylyl cyclase and PKG (Socodato *et al.* 2009).

Neuronal nitric oxide synthase is a Ca^{2+}/calmodulin-dependent enzyme activated by elevation of intracellular Ca^{2+}. NMDA receptor-associated channels are considered to serve a major pathway to provide Ca^{2+} to nNOS, because nNOS is associated with NMDA receptors via scaffold protein, postsynaptic density-95 (Calabrese *et al.* 2007). Moreover, Ca^{2+} signaling via synaptic NMDA receptors is associated with enhancement of *bdnf* gene expression in hippocampal neurons (Hardingham *et al.* 2002). We found that NMDA receptor antagonists blocked the effects of Am80 with respect to 8-nitro-cyclic GMP formation and BDNF up-regulation, indicating that NMDA receptor-mediated Ca^{2+} influx indeed plays an important role in nNOS activation leading to BDNF expression. Induction of nNOS expression by RAR stimulation was not influenced by NMDA receptor antagonists, suggesting that Ca^{2+} influx is required for activity but not expression of nNOS. Whether or not RAR stimulation enhances NMDA receptor-mediated Ca^{2+} influx remains to be determined. Because spontaneous synaptic activity drives NMDA receptor activation in midbrain slice cultures even under control conditions (Katsuki *et al.* 2003), further acceleration of NMDA receptor stimulation may not be required to cause Ca^{2+} influx to allow nNOS activation. On the other hand, retinoid signaling induced by ATRA enhances synaptic activity in hippocampal neurons (Aoto *et al.* 2008). ATRA has also been reported to up-regulate the expression of NR2B subtype of NMDA receptors in human neuroblastoma cells (Pizzi *et al.* 2002). Therefore, if similar events are involved, enhancement of NMDA receptor-mediated synaptic transmission might contribute to Ca^{2+} influx that ultimately links to BDNF up-regulation.

In the present study, we examined RAR-induced signal transduction in the absence of inflammatory stimuli. NO-cyclic GMP signal was sufficient to up-regulate BDNF expression, as 8-Br-cyclic GMP mimicked the effect of Am80. On the other hand, after treatment with interferon-γ/lipopolysaccharide, we observed that BDNF expression was down-regulated, which was reversed by concurrent treatment with Am80 (Y. Kurauchi and H. Katsuki, unpublished observations). We should note that, in this situation, substantial amount of NO and cyclic GMP is already present because inducible NO synthase is expressed in activated microglia (Kurauchi *et al.* 2009). Therefore, additional signaling mechanisms might be required for RAR stimulation to maintain BDNF expression under inflammatory conditions.

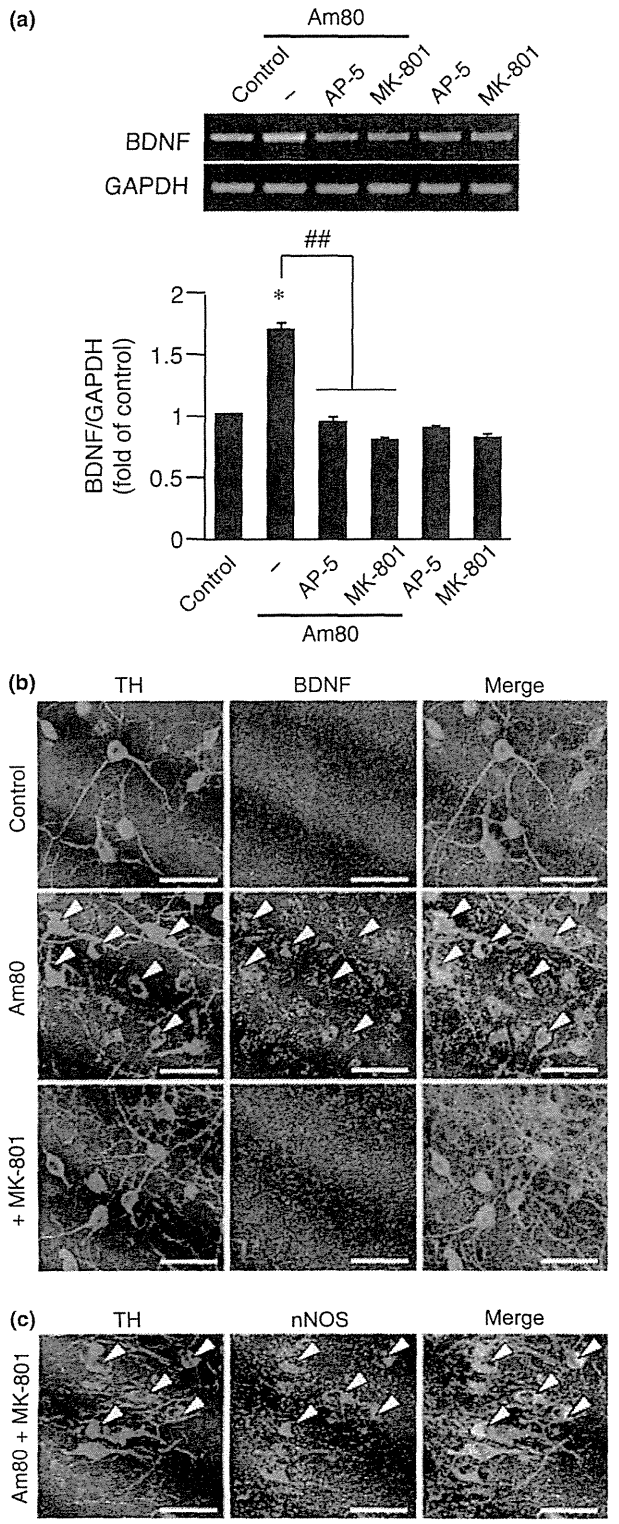

Fig. 6 NMDA receptors are involved in BDNF expression by RAR stimulation in dopaminergic neurons. (a) Effects of AP-5 (50 μM) and MK-801 (10 μM) on *bdnf* mRNA expression after 72-h treatment with 300 nM Am80. $n = 5$. $^*p < 0.05$ vs. control; $^{\#\#}p < 0.01$. (b) Double immunofluorescence histochemistry on TH (left panels) and BDNF (middle panels), and merged images (right panels) after 72-h treatment with 300 nM Am80. (c) Double immunofluorescence histochemistry on TH (left panels) and nNOS (middle panels), and merged images (right panels) after 24-h treatment with 300 nM Am80. MK-801 (10 μM) was applied concomitantly with Am80. Representative TH-positive cells with intense BDNF immunoreactivity are indicated by arrowheads. Scare bars, 50 μm.

Although retinoids have been well known to regulate expression of various neuronal genes and proteins (Mey 2006), RAR-mediated up-regulation of BDNF expression has not been hitherto reported, except for our recent study on midbrain slice culture (Katsuki *et al.* 2009). These facts imply that midbrain cells can recruit specialized signaling mechanisms in response to RAR stimulation. Indeed, we demonstrated here that nNOS induction and subsequent recruitment of cyclic GMP-related intracellular signaling linked RAR stimulation to BDNF expression. This novel cascade of signal transduction provides a clue to elucidate the roles of RAR signaling in mature CNS, and also provides important information to evaluate potential therapeutic value of RAR ligands as a new class of neuroprotective drugs targeted to Parkinson's disease.

Acknowledgement

This work was supported by grants from Itsuu Laboratory, Takeda Science Foundation and The Pharmacological Research Foundation (Tokyo), in addition to a Grant-in-Aid for Scientific Research from The Japan Society for the Promotion of Science and The Ministry of Education, Culture, Sports, Science and Technology, Japan. Y.K. was supported as a Research Fellow of The Japan Society for the Promotion of Science.

Supporting information

Additional supporting Information may be found in the online version of this article:

Figure S1. RAR stimulation increases *bdnf* mRNA expression via NO/cyclic GMP signaling pathway and MEK/ERK signaling pathway.

Figure S2. RAR stimulation increases nNOS expression and phosphorylation of ERK1/2.

Figure S3. Schematic representation of the signaling pathway linking RAR stimulation to BDNF up-regulation in dopaminergic neurons.

As a service to our authors and readers, this journal provides supporting information supplied by the authors. Such materials are peer-reviewed and may be re-organized for online delivery, but are not copy-edited or typeset. Technical support issues arising from supporting information (other than missing files) should be addressed to the authors.

References

Aoto J., Nam C., Poon M. M., Ting P. and Chen L. (2008) Synaptic signaling by all-*trans* retinoic acid in homeostatic synaptic plasticity. *Neuron* **60**, 308–320.

Calabrese V., Mancuso C., Calvani M., Rizzarelli E., Butterfield D. and Stella A. (2007) Nitric oxide in the central nervous system: neuroprotection versus neurotoxicity. *Nat. Rev. Neurosci.* **8**, 766–775.

Cañón E., Cosgaya J., Scsucova S. and Aranda A. (2004) Rapid effects of retinoic acid on CREB and ERK phosphorylation in neuronal cells. *Mol. Biol. Cell* **15**, 5583–5592.

Chen N. and Napoli J. (2008) All-*trans*-retinoic acid stimulates translation and induces spine formation in hippocampal neurons through a membrane-associated RARalpha. *FASEB J.* **22**, 236–245.

Ding Y., Qiao A., Wang Z., Goodwin J. S., Lee E. S., Block M. L., Allsbrook M., McDonald M. P. and Fan G. H. (2008) Retinoic acid attenuates β-amyloid deposition and rescues memory deficits in an Alzheimer's disease transgenic mouse model. *J. Neurosci.* **28**, 11622–11634.

Esplugues J. V. (2002) NO as a signalling molecule in the nervous system. *Br. J. Pharmacol.* **135**, 1079–1095.

Ghigo D., Priotto C., Migliorino D., Geromin D., Franchino C., Todde R., Costamagna C., Pescarmona G. and Bosia A. (1998) Retinoic acid-induced differentiation in a human neuroblastoma cell line is associated with an increase in nitric oxide synthesis. *J. Cell. Physiol.* **174**, 99–106.

Gofflot F., Chartoire N., Vasseur L., Heikkinen S., Dembele D., Le Merrer J. and Auwerx J. (2007) Systematic gene expression mapping clusters nuclear receptors according to their function in the brain. *Cell* **131**, 405–418.

Greer P. and Greenberg M. (2008) From synapse to nucleus: calcium-dependent gene transcription in the control of synapse development and function. *Neuron* **59**, 846–860.

Hardingham G. E., Fukunaga Y. and Bading H. (2002) Extrasynaptic NMDARs oppose synaptic NMDARs by triggering CREB shut-off and cell death pathways. *Nat. Neurosci.* **5**, 405–414.

Hu Y. and Russek S. J. (2008) BDNF and the diseased nervous system: a delicate balance between adaptive and pathological processes of gene regulation. *J. Neurochem.* **105**, 1–17.

Kagechika H., Kawachi E., Hashimoto Y., Himi T. and Shudo K. (1988) Retinobenzoic acids. 1. Structure-activity relationships of aromatic amides with retinoidal activity. *J. Med. Chem.* **31**, 2182–2192.

Katsuki H., Shibata H., Takenaka C., Kume T., Kaneko S. and Akaike A. (2003) *N*-Methyl-D-aspartate receptors contribute to the maintenance of dopaminergic neurons in rat midbrain slice cultures. *Neurosci. Lett.* **341**, 123–126.

Katsuki H., Okawara M., Shibata H., Kume T. and Akaike A. (2006) Nitric oxide-producing microglia mediate thrombin-induced degeneration of dopaminergic neurons in rat midbrain slice culture. *J. Neurochem.* **97**, 1232–1242.

Katsuki H., Kurimoto E. and Takemori S. *et al.* (2009) Retinoic acid receptor stimulation protects midbrain dopaminergic neurons from inflammatory degeneration via BDNF-mediated signaling. *J. Neurochem.* **110**, 707–718.

Kurauchi Y., Hisatsune A., Isohama Y. and Katsuki H. (2009) Nitric oxide-cyclic GMP signaling pathway limits inflammatory degeneration of midbrain dopaminergic neurons: cell type-specific regulation of heme oxygenase-1 expression. *Neuroscience* **158**, 856–866.

Lee S., Lee B., Lee J. W. and Lee S.-K. (2009) Retinoid signaling and neurogenin2 function are coupled for the specification of spinal motor neurons through a chromatin modifier CBP. *Neuron* **62**, 641–654.

Maden M. (2007) Retinoic acid in the development, regeneration and maintenance of the nervous system. *Nat. Rev. Neurosci.* **8**, 755–765.

Malaspina A. and Michael-Titus A. T. (2008) Is the modulation of retinoid and retinoid-associated signaling a future therapeutic strategy in neurological trauma and neurodegeneration? *J. Neurochem.* **104**, 584–595.

Masiá S., Alvarez S., de Lera A. R. and Barettino D. (2007) Rapid, nongenomic actions of retinoic acid on phosphatidylinositol-3-kinase signaling pathway mediated by the retinoic acid receptor. *Mol. Endocrinol.* **21**, 2391–2402.

Mey J. (2006) New therapeutic target for CNS injury? The role of retinoic acid signaling after nerve lesions. *J. Neurobiol.* **66**, 757–779.

Nagl F., Schönhofer K., Seidler B., Mages J., Allescher H., Schmid R., Schneider G. and Saur D. (2009) Retinoic acid-induced nNOS expression depends on a novel PI3K/Akt/DAX1 pathway in human TGW-nu-I neuroblastoma cells. *Am. J. Physiol. Cell Physiol.* **297**, C1146–C1156.

Ota K. T., Pierre V. J., Ploski J. E., Queen K. and Schafe G. E. (2008) The NO-cGMP-PKG signaling pathway regulates synaptic plasticity and fear memory consolidation in the lateral amygdala via activation of ERK/MAP kinase. *Learn. Mem.* **15**, 792–805.

Pedrini S., Bogush A. and Ehrlich M. E. (2008) Phosphatidylinositide 3-kinase and protein kinase C zeta mediate retinoic acid induction of DARPP-32 in medium size spiny neurons in vitro. *J. Neurochem.* **106**, 917–924.

Personett D., Fass U., Panickar K. and McKinney M. (2000) Retinoic acid-mediated enhancement of the cholinergic/neuronal nitric oxide synthase phenotype of the medial septal SN56 clone: establishment of a nitric oxide-sensitive proapoptotic state. *J. Neurochem.* **74**, 2412–2424.

Pizzi M., Boroni F., Bianchetti A., Moraitis C., Sarnico I., Benarese M., Goffi F., Valerio A. and Spano P. (2002) Expression of functional NR1/NR2B-type NMDA receptors in neuronally differentiated SK-N-SH human cell line. *Eur. J. Neurosci.* **16**, 2342–2350.

Sawa T., Zaki M. and Okamoto T. *et al.* (2007) Protein S-guanylation by the biological signal 8-nitroguanosine 3′, 5′-cyclic monophosphate. *Nat. Chem. Biol.* **3**, 727–735.

Shudo K., Fukasawa H., Nakagomi M. and Yamagata N. (2009) Towards retinoid therapy for Alzheimer's disease. *Curr. Alzheimer Res.* **6**, 302–311.

Socodato R., Magalhães C. and Paes-de-Carvalho R. (2009) Glutamate and nitric oxide modulate ERK and CREB phosphorylation in the avian retina: evidence for direct signaling from neurons to Müller glial cells. *J. Neurochem.* **108**, 417–429.

Umemiya H., Fukasawa H. and Ebisawa M. *et al.* (1997a) Regulation of retinoidal actions by diazepinylbenzoic acids. Retinoid synergists which activate the RXR-RAR heterodimers. *J. Med. Chem.* **40**, 4222–4234.

Umemiya H., Kagechika H. and Fukasawa H. *et al.* (1997b) Action mechanism of retinoid-synergistic dibenzodiazepines. *Biochem. Biophys. Res. Commun.* **233**, 121–125.

Wong L.F., Yip P. K. and Battaglia A. *et al.* (2006) Retinoic acid receptor β2 promotes functional regeneration of sensory axons in the spinal cord. *Nat. Neurosci.* **9**, 243–250.

Zetterström R. H., Lindqvist E., Mata de Urquiza A., Tomac A., Eriksson U., Perlmann T. and Olson L. (1999) Role of retinoids in the CNS: differential expression of retinoid binding proteins and receptors and evidence for presence of retinoic acid. *Eur. J. Neurosci.* **11**, 407–416.

Nitric Oxide 25 (2011) 169–175

Contents lists available at ScienceDirect

Nitric Oxide

journal homepage: www.elsevier.com/locate/yniox

Methodological proof of immunochemistry for specific identification of 8-nitroguanosine 3′,5′-cyclic monophosphate formed in glia cells

Hideshi Ihara [a,*,1], Ahmed Khandaker Ahtesham [b,1], Tomoaki Ida [a], Shingo Kasamatsu [a], Kouhei Kunieda [a], Tatsuya Okamoto [b], Tomohiro Sawa [b], Takaaki Akaike [b]

[a] Department of Biological Science, Graduate School of Science, Osaka Prefecture University, Sakai, Osaka 599-8531, Japan
[b] Department of Microbiology, Graduate School of Medical Sciences, Kumamoto University, Kumamoto 860-8556, Japan

ARTICLE INFO

Article history:
Available online 3 May 2011

Keywords:
8-Nitroguanosine 3′,5′-cyclic monophosphate
8-Nitroguanine
Immunocytochemistry
Soluble guanylate cyclase
Reactive nitrogen oxide species

ABSTRACT

The biological significance of nitrated guanine derivatives, especially 8-nitroguanosine 3′,5′-cyclic monophosphate (8-nitro-cGMP), has become evident. Therefore it is important to determine the presence and relative abundance of 8-nitro-cGMP formed in cells and tissues. In the present study, we performed immunocytochemistry with monoclonal antibodies specific for 8-nitroguanine (clone NO2-52) and 8-nitro-cGMP (clone 1G6) in rat C6 glioma cells and rat primary cultured astrocytes. Immunocytochemistry utilizing the anti-8-nitro-cGMP monoclonal antibody (1G6) indicated that immunostaining increased markedly in C6 cells expressing increased amounts of inducible nitric oxide synthase (iNOS) after treatment with lipopolysaccharide (LPS) plus cytokines. Treatment of C6 cells with inhibitors for NOS and soluble guanylate cyclase (sGC) completely nullified the elevated 1G6 immunoreactivity. These results were consistent with the liquid chromatography-tandem mass spectrometry (LC-MS/MS) analyses. Immunocytochemistry performed using NO2-52 also showed that treatment of cells with inhibitors for NOS and sGC completely nullified the elevated immunoreactivity; this indicated that 8-nitro-cGMP is a major component of 8-nitroguanine derivatives produced in cells. Similar results were obtained in the primary astrocytes stimulated with LPS plus cytokines. Because immunocytochemistry is a conventional, powerful, and fairly straightforward method for determining the presence, localization, and relative abundance of an antigen of interest in cultured cells, anti-8-nitroguanine (NO2-52) and anti-8-nitro-cGMP (1G6) antibodies could be useful tools for analyzing nitrated guanine nucleotides, especially 8-nitro-cGMP, by means of immunocytochemistry.

Introduction

Nitric oxide (NO) has diverse physiological functions in vascular regulation, neuronal transmission, inflammation, and cell death [1–4]. The major NO pathway is mediated by the activation of soluble guanylate cyclase (sGC), which leads to production of guanosine 3′,5′-cyclic monophosphate (cGMP) [5]. However, it has been suggested that there also exist NO-related biological phenomena that are not necessarily caused by cGMP [6–8]. These phenomena include chemical modification of biomolecules, including nitrosylation and nitration of amino acids, proteins, and lipids, and such modification is induced by NO-derived reactive nitrogen oxide species (RNOS), such as peroxynitrite ($ONOO^-$) and nitrogen dioxide (NO_2) [6–8].

RNOS induces nitration of nucleic acids in addition to that of amino acids, proteins and lipids [9–11]. Nitrated guanine derivatives, including 8-nitroguanine and 8-nitroguanosine, were formed in cultured cells and in tissues from murine viral pneumonia and human lung disease [9–11]. We recently discovered that a novel nitrated cyclic nucleotide, namely, 8-nitroguanosine 3′,5′-cyclic monophosphate (8-nitro-cGMP), is generated in an NO-dependent manner [12]. 8-Nitro-cGMP exhibited the strongest redox activity among the examined nitrated guanine derivatives; this activity was different from that which activate cGMP-dependent protein kinases [12]. Because 8-nitro-cGMP possesses an electrophilic property, it

Abbreviations: iNOS, inducible nitric oxide synthase; sGC, soluble guanylate cyclase; cGMP, guanosine 3′,5′-cyclic monophosphate; 8-nitro-cGMP, 8-nitroguanosine 3′,5′-cyclic monophosphate; RNOS, reactive nitrogen oxide species; LC-MS/MS, liquid chromatography-tandem mass spectrometry; Keap1, Kelch-like ECH-associated protein 1; L-NMMA, N^{ω}-monomethyl-L-arginine; LPS, lipopolysaccharide; IFN-γ, interferon-γ; TNFα, tumor necrosis factor α; IL-1β, interleukin-1β; DMEM, Dulbecco's modified Eagle's medium; NEM, *N*-ethylmaleimide; PBS, phosphate-buffered saline; SDS, sodium dodecyl sulfate; PAGE, polyacrylamide gel electrophoresis; BSA, bovine serum albumin; HPLC, high performance liquid chromatography; S.E., standard error; ECD, electrochemical detection.

* Corresponding author. Address: 1-1 Gakuen-cho, Sakai, Osaka 599-8531, Japan. Fax: +81 72 254 9753.
E-mail address: ihara@b.s.osakafu-u.ac.jp (H. Ihara).
[1] These authors contributed equally to this work.

1089-8603/$ - see front matter © 2011 Elsevier Inc. All rights reserved.
doi:10.1016/j.niox.2011.04.015